Human occupation and environmental change in the western Maghreb during the Last Glacial Maximum (LGM) and the Late Glacial. New evidence from the Iberomaurusian site Ifri El Baroud (northeast Morocco)

Human occupation and environmental change in the western Maghreb during the Last Glacial Maximum (LGM) and the Late Glacial. New evidence from the Iberomaurusian site Ifri El Baroud (northeast Morocco)

Alessandro Potì [a], *, Martin Kehl b, Manuel Broich [a], Yolanda Carrión Marco [c], Rainer Hutterer [d], Thalia Jentke [d], Jörg Linstädter [e], José Antonio López-Sáez [f], Abdeslam Mikdad [g], Jacob Morales [h], Sebastián Pérez-Díaz [f], Marta Portillo [i], Clemens Schmid [j], Paloma Vidal-Matutano [h], [k], Gerd-Christian Weniger [a], [l]

[a] University of Cologne, Institute of Prehistoric Archaeology, Albertus-Magnus-Platz, 50923 Cologne, Germany
[b] University of Cologne, Institute of Geography, Albertus-Magnus-Platz, 50923, Cologne, Germany
[c] University of Valencia, Department of Prehistory, Archaeology and Ancient History, Av. Blasco Ibáñez 28, 46010 Valencia, Spain
[d] Zoologisches Forschungsmuseum Alexander Koenig, Adenauerallee 160, 53113 Bonn, Germany
[e] German Archaeological Institute, Kommission für die Archäologie Außereuropäischer Kulturen (KAAK), Dürenstraße 35-37, 53173 Bonn, Germany
[f] Institute of History, National Council of Scientific Research (CSIC), Albasanz 26-28, 28037 Madrid, Spain
[g] Institut National des Sciences de l'Archéologie et du Patrimoine (INSAP), Hay Riad, Madinat Al Irfane, Angle rues 5 et 7, 10000 Rabat, Morocco
[h] University of Las Palmas de Gran Canaria, Departamento de Ciencias Históricas, Pérez del Toro 1, 35003 Las Palmas, Spain
[i] University of Reading, Department of Archaeology, School of Archaeology, Geography and Environmental Sciences, Whiteknights, Reading RG6 6AB, UK
[j] University of Kiel, Institute of Pre- and Protohistoric Archaeology, Johanna-Mestorf-Straße 2-6, 24118 Kiel, Germany
[k] Université Cote d'Azur, CEPAM, UMR 7264, 24 avenue des Diables Bleus, 06357 Nice, France
[l] Neanderthal Museum, Talstraße 300, 40822 Mettmann, Germany

Abstract

With the onset of the Last Glacial Maximum (LGM), hunter-gatherers of the so-called Iberomaurusian techno-complex appeared in what is now the Mediterranean Maghreb. During a period of about seven thousand years, these groups left sandy occupation layers in a limited number of archaeological sites, while at the beginning of Greenland Interstadial (GI) 1, the sudden shift towards the deposition of shellrich sediments and the increase in number of sites document clear changes in subsistence strategies as well

as occupation density. It is highly likely that these shifts in human behaviour are related to paleoenvironmental changes in the area, which, so far, are poorly documented in geological and archaeological archives. Ifri El Baroud (Gunpowder Cave, northeast Morocco) contains a well-stratified archaeological sequence covering both phases of Iberomaurusian occupation separated by a sharp sedimentary change. In this paper, new chronological data and detailed investigations on site formation using sedimentology and micromorphology are presented. In addition, results of the analyses of fauna, pollen, macrobotanical remains, and phytoliths are included. This data contributes to a full-scale paleoenvironmental interpretation of the site's archaeological deposits, highlighting the fluctuations of landscape conditions at the transition from the cold-arid Greenland Stadial (GS) 2.1 to the warmer and moister Greenland Interstadial 1.

1. Introduction

The late upper Palaeolithic in northwest Africa is represented by the Iberomaurusian techno-complex (Pallary, 1909), a bladelet industry with backed pieces that has been described in many sites along the coast of the Maghreb and Libya as well as in the Atlas Mountains (Balout, 1955; McBurney, 1967). Based on new AMS radiocarbon dates, the Iberomaurusian appeared for the first time across the Maghreb at about 25-23 ka calibrated years BP (cal BP) (Barton et al., 2013; Hogue and Barton, 2016) and continued until the end of the Pleistocene (Bouzouggar et al., 2008).

Despite the long duration of the techno-complex, only a handful of sites display long and complete sequences that document human occupations between the Last Glacial Maximum and the Younger Dryas in detail. Indeed, the archaeology of the early Iberomaurusian (25/23-16 ka cal BP) only comes from a very restricted number of sites, which entails a serious lack of information for the initial phases of occupation (Potì and Weniger, in press).

Only after Heinrich Event 1 (*sensu* Fletcher and Sánchez-Goñi, 2008), with the climatic ameliorations of the Greenland Interstadial (GI) 1 (around 16-15 ka cal BP), the amount of data increases throughout northwest Africa (Linstädter et al., 2012). During this warmer and moister phase, substantial changes occurred in many aspects of human behaviour and settlement dynamics (Barton et al., 2013, 2016). One of these is represented by the rapid accumulation of massive midden deposits composed of high

proportions of land-snail shells (so-called escargoti_eres) (Nami and Moser, 2010) that seems to document an important change insubsistence strategy. Aspects of technical discontinuity can be observed between the lithic industries prior to the GI 1 and those in the Interstadial, revealing a strict relationship between environment fluctuations and behavioural changes (Potì, 2017).

Nevertheless, given the scarcity of stratigraphic sequences covering long intervals of time, considerable difficulties surround the clear understanding of the Iberomaurusian adaptive strategies and the landscape dynamics in the Late Pleistocene Maghreb. Although significant progress has been made in the last decade (Barton et al., 2016), there is undoubtedly a need for additional data. In this patchy archaeological scenery, one of the possibly most informative and well-preserved Iberomaurusian sequences is found at the site Ifri El Baroud, in the mountainous northeast Morocco (Nami, 2007). The site contains a finely stratified sequence of charcoal-rich occupational layers with faunal and lithic finds that attest to repeated Iberomaurusian occupations between the LGM and the Younger Dryas.

As part of resumed research work at the site, a new long excavation was conducted in 2015. The primary purpose was to reexplore the Iberomaurusian deposit in its entirety and collect new high-resolution samples for a detailed chronological and palaeoenvironmental study. In this article, we report the chronology for the stratified archaeological sequence of Ifri El Baroud based on a new set of AMS radiocarbon dates. In addition, we provide results of micromorphological and sedimentological analyses of the site's deposits that highlight sedimentary and anthropological events involved in the formation processes. Local vegetational patterns and environmental conditions are reconstructed based on integrated analyses of environmental indicators including both micro- and macrobotanical material (pollen, seeds, charcoal, opal phytoliths, and calcitic plant microfossils) and faunal remains (molluscs, micro- and macrofauna).

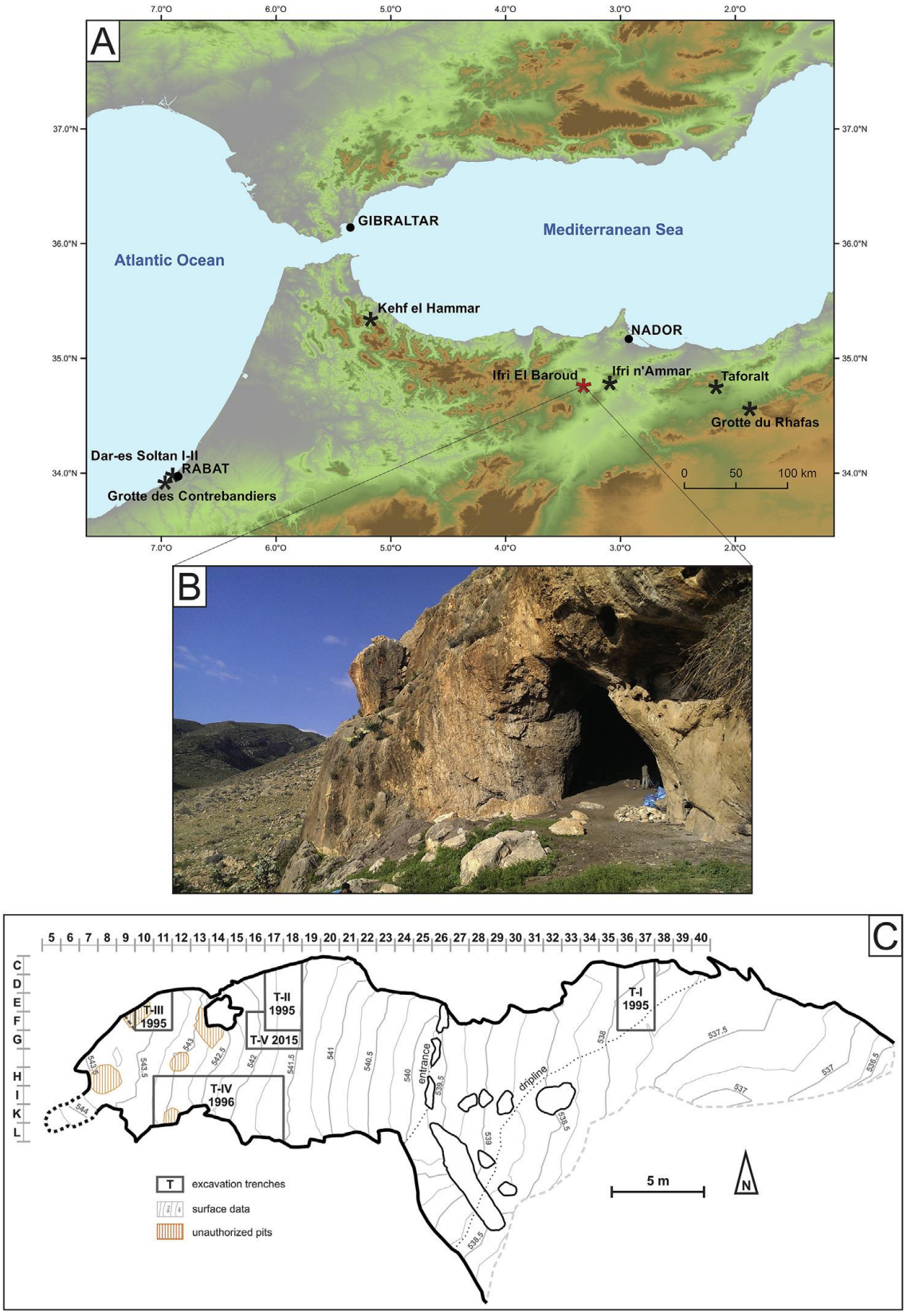

Fig. 1. (A) Map showing the location of Ifri El Baroud in northeast Morocco and other Iberomaurusian sites. (B) An external view of the cave taken in 2015. (C) Plan of the cave showing the position of the excavated trenches.

2. The site and its regional setting

Ifri El Baroud ("Gunpowder Cave") is located 539m above mean sea level at the foot of the Ich Chaboun Massif in the province of Guercif, northeast Morocco (34°45/N, 3º18/W), approx. 50 km inland from the current Mediterranean coast. The cave is a large and elongated karst chamber with one single entrance oriented towards the east (Fig. 1). From its position it opens on the plain of Guerouaou, a large alluvial depression (currently ~380m amsl) that acts as a natural crossroads between the Mediterranean coast and the Middle Atlas, and between the Eastern Rif Mountains and the Moulouya River Basin (Nami and Moser, 2010). The geology of the region is dominated by Jurassic and Cretaceous carbonate rocks (mainly limestone and dolomite), and Neogene to Quaternary deposits, while volcanic rocks crop out in limited areas.

The cave is about 22m deep, 11m wide and 13m high from the actual surface to the highest point of the roof. The bedrock irregularly slopes towards the entrance, with a difference in height of about 4mfrom the back to the front of the cave. This morphological setting favoured the accumulation and preservation of sediments in specific points of the chamber that are less affected by alteration processes, for example against the north wall or in other more depressed loci (Potì, 2017). Towards the entrance of the cave, a significant volume of archaeological deposits has leached outwards due to the action of water, wind and anthropic factors.

Today, Ifri El Baroud lies within the natural area of Gareb (Valdés et al., 2002, 2006). The meteorological data for the city of Saka, which is about 19 km SSW from the site, show an average annual temperature of 16 ºC and 340mm of precipitation, and are indicative of a thermo-Mediterranean biogeographical zone with precipitation typical of a semi-arid climate (Rivas-Martínez, 1987). The current vegetation around the site is treeless, mainly composed by annuals and some perennials shrubs such as *Stipa tenacissima* and *Capparis spinosa*.

3. Research history

First excavations at the site were undertaken in 1995 by a team from the Institut National des Sciences de l'Archéologie et du Patrimoine of Rabat (INSAP) and the Commission for the Archaeology of non-European cultures of the German Archaeological Institute of Bonn (KAAK) (Mikdad et al., 2000). At that time, archaeologists excavated three test trenches (labelled I, II, III) along the north wall of

the cave. The excavations enabled the identification of a thick sequence of Iberomaurusian deposits very rich in charcoal and archaeological finds. The Iberomaurusian deposits appeared to be particularly well preserved in the central-inner part of the cave. Trench II provided the deepest and most complete sequence, reaching approx. 3 m depth and showing a well-preserved succession of Iberomaurusian occupation horizons. These included a lower reddish-brown, finely layered sedimentary succession (named "Couche rouge") and an upper greyish shell midden deposit named "Escargotière") (Potì, 2017). In the inner part of the cave, in trench III, the sediment extended to a depth of approx. 2.2 m. At *ca*. 1.4m below the surface, at the base of the midden sediments, an Iberomaurusian burial of an adult female was identified and excavated (Ben-Ncer, 2004). In this part of the chamber, the excavation also exposed a small-size brownish deposit of Epipalaeolithic and Neolithic origin (first ~30-40 cm) overlying the Iberomaurusian. On the uppermost levels, ceramic fragments have been found in primary position, but the deposit seemed in part to have been disturbed by subsequent events. In the other sectors of the cave, sediments younger than Iberomaurusian had been removed in the past by natural and anthropic events, and therefore only single objects without stratigraphic context could be recorded, among them some early Neolithic sherds (Mikdad and Eiwanger, 1995; Nami, 2001). Finally, outside the cave, archaeological deposits in test trench I showed to be less than 0.8mdeep and mainly composed of Iberomaurusian-Epipalaeolithic greyish sediment rich in limestone rubble and apparently without snail shells (Nami, 2001).

Archaeological investigation continued in 1996 with the excavation of a larger area, trench IV, along the south wall of the cave. The new trench revealed a good preservation of Iberomaurusian layers down to a maximum depth of 2.8m in the easternmost part, but also sectors characterized by disturbances and sub-recent deposits. In the inner part of the trench, remnants of Epipalaeolithic- Neolithic layers were recorded within the first 40e45 cm, but also in this case they appeared to have partially been contaminated by recent activities (Nami, 2001, 2007). The Iberomaurusian sequence uncovered in trench IV showed the same stratigraphic evolution as recorded in trench II and III, with the main progression from lower reddish-brown fine sediment to the greyish midden deposits. During the 1995 and 1996 field seasons, only dry sieving of the sediments could be employed, resulting in a limited recovery of small organic and inorganic remains (Potì, 2017). However, in 1996e1997, a series of charcoal samples

collected during the excavation of trenches II, III and IV was submitted to the radiocarbon laboratory of Berlin and dated conventionally (Görsdorf and Eiwanger, 1999). The dates obtained ranged approximately from 20 ka to 13 ka cal BP, indicating an exceptionally long and continuous occupation of the cave. On the base of this absolute chronology, two main cultural components could be established at the site. The earliest component corresponds to the "early Iberomaurusian" occupation of the lower units identified in trenches II, III and IV (Couche rouge, roughly >20-16. ka cal BP). The second, more recent, corresponds to the "late Iberomaurusian", equivalent to the occupation with midden layers (Escargotière, roughly 15.5-13 ka cal BP). In addition, two dates from the laboratory of Berlin (Bln-4755 and Bln-4872) plus two other samples delivered to the AMS laboratory of Kiel (KIA-510-I and KIA-511-I) confirmed the presence of remnant Holocene deposits in the inner part of the cave as well as sub-recent events (Görsdorf and Eiwanger, 1999).

After 20 years, research at the sitewas resumed in 2014-2015 in the framework of a joint research project between the Collaborative Research Centre 806 - Our Way to Europe (Universities of Cologne, Bonn, Aachen, Neanderthal Museum) and the INSAP. In 2014, a preliminary inspection attested the good state of conservation of the site. The continuous frequentation of the cave by local flocks and herds favoured the formation of a superficial dung-rich deposit that protected the underlying archaeological deposits. Nevertheless, the inner part of the cave appeared heavily damaged by several clandestine pits especially focused around the area of trench III (Potì, 2017). In 2015, a new excavation targeted the central part of the site, where the much deeper and richer stratigraphic sequence is preserved. The newly investigated area has been named "trench V". The excavation was intended to be an enlargement of trench II, as to obtain comparative samples with the earlier test excavations and expand the network of stratigraphic correlations. During the excavation, as the depth increased, the working area was reduced for security reasons, leaving progressive steps on the profiles. Due to this, the planum at the base of the trench measured only *ca*. 2m^2 from the starting 5m^2. Bedrock was reached at a depth of approx. 3m, at the same level reached in trench II in 1995.

4. Materials and methods

The interpretation of the archaeological sequence of Ifri El Baroud results from the combination of the data collected during the 1995 and 1996 field campaigns with the observations made during the excavation of trench V in 2015, which involved the reconsideration and the new description of the whole sequence, as well as detailed textural and micromorphological analysis. Already at the beginning of the field work in 2015, it was possible to partially reconstruct the measurement grid of the 1995 and 1996 campaigns to achieve a high degree of comparability between old and new stratigraphic observations.

4.1. Excavation in 2015 and sediment sampling

All layers have been described based on colour, consistence, sedimentation mode, stratigraphic features, and variation in the amount and distribution of ash, snail shells, charcoal and archaeological content. The profiles and plana were recorded with technical drawings and orthoimages.

The archaeological sequence of Ifri El Baroud consists of several superimposed and juxtaposed layers with rather homogeneous and recurring sedimentary features that allow them to be sorted into discrete macro-groups (units). Their formation processes are considered collectively (see further). Therefore, we used the term "unit" to describe a package of strata which show undifferentiated features in terms of components, consistence, and main colour, and thus reflect similar depositional conditions (Potì, 2017).

The excavation of trench V was performed with artificial spits on a 0.25m^2 grid, trying to respect the complex structure of the stratigraphic succession. However, this was not always possible. While the shape of the boundary between upper midden and lower brown-reddish sediments (i.e. Escargotière e Couche rouge limit) was carefully explored, one of the most complicated and challenging parts of the excavation was the removal of the upper shellrich deposits. Although midden layers can be quite thick (up to 20-25 cm for the snail lenses), they are generally characterized by a limited lateral extension and irregular geometry, resulting in complex horizontal relationships and difficulties in the correlation of e even rather close e profiles (Potì, 2017). This stratigraphic context is further complicated by the extremely loose cohesion of the sediments, their powdery appearance and homogeneous greyish colour. It proved impossible to follow every single layer of sediment or each snail lens. However, the

tracking of individual features and lenses or visible limits was practised whenever possible, separating sediments during the excavation.

To estimate the attribution of artefacts recovered during the 2015 campaign to the main stratigraphic units, the three dimensional architecture of these units was reconstructed computationally. Stratigraphic limits were inferred from profile observations and analysed in relation to the artificial excavation spits. Even the macro-units were at times challenging to trace during the excavation, but they became very obviously visible in the final profile analysis at the end of the campaign. To retrieve this information and make it again useful to understand the stratigraphic attribution of the excavation squares e and therefore the artefacts within them e we used 3D surface reconstruction via Kriging to extrapolate the unit borders from the profiles over the extent of the narrow trench. Based on this, a dedicated algorithm was able to calculate the degree of membership of every square to every unit. This method allowed to cross-check the correlation between natural units and artificial squares, and to identify the border cases where the correlation was not completely clear. These cases are of questionable value for chronotypological analysis and had to be singled out for careful assessment. Code and data for the semiautomatic square allocation are available in a small research compendium (Schmid, 2019) and an R package on CRAN (https://CRAN.R-project.org/package-recexcavAAR) along with a technical description of the process in a vignette.

The sedimentary features of the layers recognized in trench V can be considered as descriptive of the total deposits of the cave and can therefore be “projected” on the profiles of the other sectors. No Epipalaeolithic or Neolithic deposits were found during the excavation of trench V. Accordingly, the geo-archaeological description of these levels only comes from the information reported in the field diaries of 1995 and 1996. During the excavation of trench V, bucket flotation was performed for all removed sediments. This method has allowed the recovery of important environmental indicators such as macrobotanical materials (charcoal, seeds), snail shells and microfaunistic remains.

At the end of the field campaign, sediment samples were collected for sedimentological, pollen and phytoliths analyses. The sediment samples were extracted from two columns on the main profiles of trench V, namely the south (IBS) and west (IBW) profile (Fig. 2). The south profile documents the middle-upper part of the

stratigraphy, while the west profile documents the medium-low part. Both sediment columns were sampled from bottom to top at intervals of up to 5 cm, taking care not to mix separate layers and features. All sediment levels defined in the field were included in the sampling, with a total of 29 samples from the south profile and 32 from the west profile.

4.2. Sedimentology

Sedimentological analysis was performed at the Institute of Geography of the University of Cologne. After drying at 40 ºC, the size fraction greater than 2 mm in diameter was separated by dry sieving and the fine fraction (<2 mm) was divided into three subsamples used for sedimentological, palynological and phytolith analyses. Sediment colour was determined by measuring the diffused reflected light in the range from 360 to 740 nm using a Konica Minolta CM-5 spectrophotometer. The obtained spectral information was converted to the CIE colour space (L*, a*, b*) (CIE 1978), utilizing the SpectraMagic NX software (Konica Minolta). The L* values represent the luminance of the sample ranging from L*0 (maximum extinction of light, black) to L*100 (maximum luminance, white). Positive a* and b* values indicate redness and yellowness, respectively, while negative values represent greenness (a*) and blueness (b*).

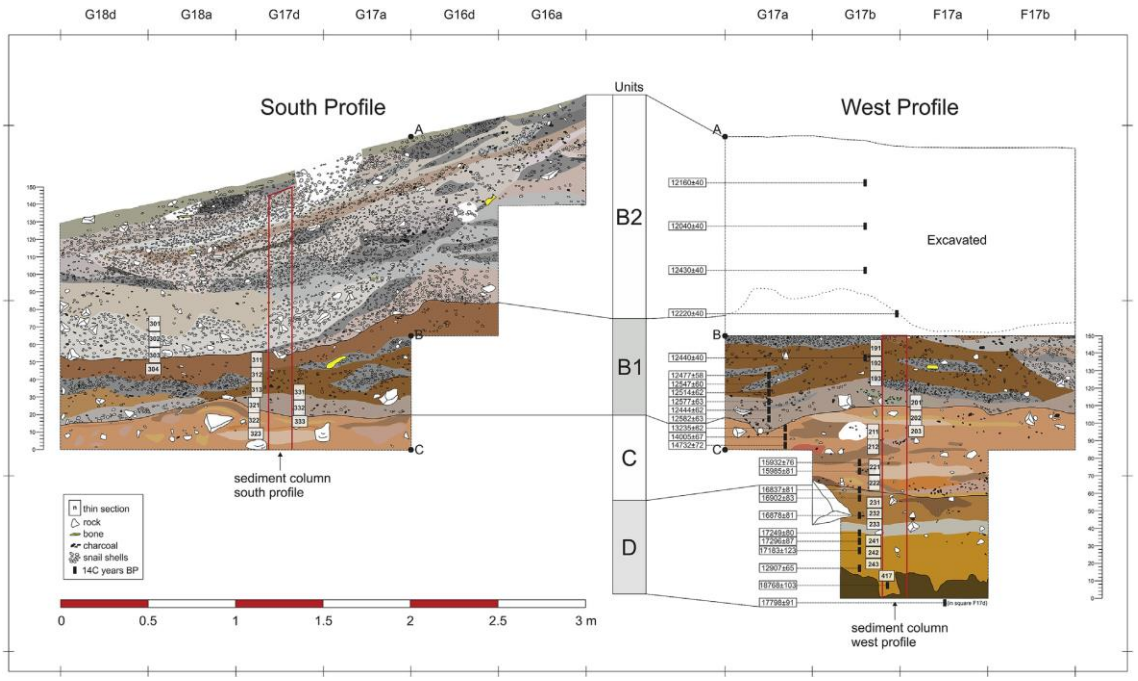

Fig. 2. Stratigraphy of Ifri El Baroud: south profile (IBS) and west profile (IBW) of trench V. The picture displays the division into units and the position of radiocarbon and micromorphology samples as well as columns of sediment sampling.

The contents of total carbon (TC), total nitrogen (TN) and total organic carbon (TOC) were measured with element analyses using a Vario EL Cube (Elementar Analysesysteme GmbH, Hanau, Germany). Prior to measuring, samples were ground and homogenized in an agate mortar. Measurement of TOC was carried out after destruction of carbonates using hydrochloric acid (HCl, 10%). Total inorganic carbon (TIC) was derived from the difference between TC and TOC. The amount of carbonates was expressed as calcium carbonate equivalent (CCE) by multiplying TIC with 8.3331. As an estimate for the amount of organic matter (OM), TOC values were multiplied by 2.

4.3. Micromorphology

Ten intact sediment blocks were sampled from key points of the stratigraphic succession, including the transition from the lower reddish-brown sandy sediments to the upper greyish midden, which was well visible in the profiles of trench V. Monoliths were removed after application of plaster bandages on the outer half and subsequently wrapped.

Thin sections were prepared at the laboratory of Thomas Beckmann in Schwülper (Germany) after impregnation with resins and hardeners. Twenty-nine thin sections (80mm× 60 mm, 25-µm-thick) out of the ten sediment blocks were obtained (Fig. 2). Thin sections were observed under a polarizing microscope using plane polarized light (PPL), crossed polarized light (XPL) and oblique incident light (OIL), with a magnification from 20× to 500×. In addition, flatbed images at a resolution of 1200 dpi were analysed at low resolution. The description of thin sections followed the guidelines of Stoops (2003).

4.4. Radiocarbon

During the 2015 campaign, new samples of wood charcoal and burnt seeds for radiocarbon dating were recovered during flotation. Between 2016 and 2017, twenty selected samples were sent for dating to the 14C AMS Laboratory of the University of Cologne and five additional samples were sent to the AMS Laboratory of Beta

Analytics in Miami. Measurements were completed after pretreatment with the Acid-Alkali-Acid (AAA) protocol which involves the chemical cleaning of the charcoal by progressive washes first with hydrochloric acid (HCl), then with sodium hydroxide (NaOH) and again with hydrochloric acid (HCl). The new samples are added to the twenty-seven radiocarbon dates obtained from the excavations of 1995 and 1996 (Görsdorf and Eiwanger, 1999). The calibration of all 14C dates was accomplished using CalPal software (Weninger and Joris, 2008) and Intcal13 calibration curve (Reimer et al., 2013). In addition, as part of the analysis of radiocarbon dating, OxCal v4.3.2 (Bronk Ramsey, 2019) was applied to run Bayesian modelling and outlier tests assuming that each sample has a 5% prior probability of being an outlier within the General ttype Outlier Model (Bronk Ramsey, 2009). The Bayesian model incorporates only the dated samples from the Iberomaurusian units of trench V and II and the dated samples from unit A of trench III and IV.

4.5. Macrobotanical remains

Anthracological analysis was performed at the Department of Prehistory, Archaeology and Ancient History of the University of Valencia. For this study, charcoal samples were selected from the sediment column of sub-squares G17a, G17b, G17c and G16a based on its higher stratigraphic reliability (Carrión Marco et al., 2018). A total of 6920 L of sediment were processed by the flotation system, which made it possible to recover seeds, charcoal and other tiny plant materials included in the light fraction. Flots were sorted using a column of sieves with mesh sizes of 2, 1, 0.5, 0.25, and 0.1 mm. Charred botanical remains were very abundant and well preserved. Charcoal analysis was based on the botanical identification of carbonised wood. Each fragment was examined under a reflected light brightfield/darkfield optical microscope with different lenses ranging from 50x to 1000x magnification. The anatomical structure of taxa was compared with specialised literature on plant anatomy (among others Greguss, 1955, 1959; Jacquiot, 1955; Jacquiot et al., 1973; Neumann et al., 2001; Schweingruber, 1976, 1990) and the modern reference collection of charred wood from the Laboratory of Prehistory, Archaeology and Ancient History of the University of Valencia. For the observation of specific features and to take photos, we used a Hitachi S-4100 scanning electron microscope (SEM) located at the Central Service for Experimental Research

Support (SCSIE) at the University of Valencia. The nomenclature used was that of Flora Europaea (Tutin et al., 1964).

The analysis of seed remains was carried out on almost all the sediments excavated in trench V. Charred remains of seeds and fruits were collected from 376 sediment samples through a flotation machine and with a 0.5mm sieve. The floating fraction of each sample was dried and then filtered in a column of sieves with 2, 1,and 0.5mm meshes. Plant remains were individualised and determined by means of a binocular microscope at magnifications between 8x and 80x. Plant taxa identification was carried out by comparing the archaeological specimens with modern seeds and fruits from the reference collection of the Department of Historical Sciences, University of Las Palmas de Gran Canaria, Spain. Furthermore, a seed atlas and other specialised literature on the flora of Morocco also served to identify the plant remains (Charco, 2001; Fennane et al., 1999, 2007, 2014).

4.6. Palynology

Palynological analysis was performed at the Institute of History (CSIC) of Madrid. For the pollen analysis presented here, 32 samples from west profile (150-0 cm) and 18 from south profile (150-55 cm) were considered. Pollen preparation (10 g per sample) followed standard methods in archaeopalynology (Burjachs et al., 2003) using treatment with HCl, 10% KOH, HF and concentration with Thoulet liquor, although acetolysis was not carried out to allow the identification of any contamination by modern pollen. The final residue was suspended in glycerine and counted until a pollen sum of 250 pollen grains was reached. Aster type, Cardueae and Cichorioideae with possible zoophily were also excluded (López-Sáez et al., 2003). Slides were examined with a light microscope using a magnification of 400× or 1000×. Pollen taxonomy follows Moore et al. (1991), Reille (1992) and Valdés et al. (1987). *Pinus pinaster* and *Pistacia lentiscus* pollen differentiation followed Burgaz et al. (1994) and Carrión et al. (2000). The pollen diagram was drawn using Tilia 2.0 and TGView (Grimm, 1992, 2004). The terms ‘local’ (0-20 m), ‘extra-local’ (20 m-2 km) and ‘regional’ (2e200 km) used in the text refer to different pollen source areas according to Prentice (1985).

4.7. Phytoliths

Phytolith analysis was performed at the Palaeobotany Laboratory Lydia Zapata (Department of Geography, Prehistory and Archaeology) and the Department of Analytic Chemistry of the University of the Basque Country. Thirty-two sediment samples from profiles IBS and IBW were selected for the study. Phytolith extraction followed the methods of Katz et al. (2010). A minimum of 200 phytoliths with recognizable morphologies were examined at 200× and 400× using a Nikon Eclipse 50i optical microscope. Morphological identification was based on modern plant reference collections (Albert and Weiner, 2001; Albert et al., 2008, 2016; Portillo et al., 2014) and standard literature (Brown, 1984; Mulholland and Rapp, 1992; Piperno, 2006; Twiss, 1992). The terms used to describe phytolith morphologies follow the standards of the International Code for Phytolith Nomenclature (Madella et al., 2005).

4.8. Faunal remains

The analysis of the faunal remains was carried out at the Zoologisches Forschungsmuseum Alexander Koenig (ZFMK) in Bonn, Germany. Due to the high amount of faunal material from the entire excavation of 2015, only macrofaunal remains, i. e. bones and teeth, from one square metre (i.e. from four neighbouring sub-squares G17a, b, c, d) were identified and analysed. In addition to this material, some special finds from other sub-squares and the surface (nettoyage), documented during first examinations in the field were also analysed. The selected material was studied in detail using the comparative skeletal material collection of the museum and additional anatomical literature by Goody (2004) and Popesko (2007) as well as drawings of Pales and Lambert (1971). Some of the complete or nearly complete bones were measured after the method described in von den Driesch (1976) and Peters et al. (1997). For the selected sub-squares, all indeterminable vertebrate bone fragments and ostrich eggshell fragments were weighed for quantitative analyses.

Microfauna (small mammals, birds, amphibians, reptiles) and shells of gastropods were studied from the sediment column of sub-square G17b (spits 1 to 53). Samples were identified with the help of a stereomicroscope Wild M5 at the ZFMK. For the identification of species, specimens from the vertebrate reference collection of the Museum were used for comparison. Sediments of lower units were densely packed with massive structure. Shell and bone fragments from the lower levels (spits 31e53) were often included in small hard soil aggregates/blocks which were difficult to solve in

water. A solution of weak acetic acid was used to soften the hard soil chunks and recover the fossil bones included in them; this procedure was repeated several times before examination of the remnants. All components were weighed. Shells were identified as in previous studies (Hutterer et al., 2014).

5. Results

5.1. The archaeological and sedimentary sequence

Considering all sedimentary features so far identified as well as the radiocarbon chronology and archaeological variability, the Ifri El Baroud sequence has been divided into four major chronostratigraphic units, named from A to D from top to bottom (Potì, 2017). These units connect all trenches across the cave and are sealed by a surface crust of a sub-recent, dung-rich anthropogenic deposit. In the following, we provide descriptions of the whole sequence, summarizing results obtained from previous excavations and the new data obtained in this study derived from analyses of the profiles of trench V (Fig. 2).

From the archaeological standpoint, the units are related to the remains of the Epipalaeolithic-Neolithic deposit (unit A) and to the Iberomaurusian deposits (units B-C-D). Regarding internal properties, each unit represents a superordinate group of layers that show similar chronostratigraphic position, recurrent macroscopic sediment features and anthropogenic signals (Potì, 2017). These groups of layers therefore appear to acknowledge similar depositional conditions in terms of both natural and anthropic events/ inputs.

The four macro-units are separated by disconformities (possibly erosive surfaces) or marked variability (sedimentological, chronological or archaeological) and are described as follows:

Unit A: remains of undifferentiated Epipalaeolithic and Neolithic deposits. Originally, this Holocene unit probably covered large parts of the cave, but it now appears to be almost completely removed by erosion. It is preserved only in the very inner part of the

cave, even though it is no thicker than 40-45 cm (west profile of trench IV). Clandestine pits and modern surface disturbances furthermore affected the preservation of the residual sediments. It is a light brownish-grey silty and partially sandy anthropogenic

deposit, loosely packed and comparatively rich in ash and charcoal. Few crushed snail shells and diffuse angular limestone rubble are present. Faunal remains are generally not well preserved due to post-depositional disturbance (actions of water, animals and humans). Layers of unit A show a sub-horizontal orientation and gently follow the slope of the modern surface. The lower sediment boundary is gradual, i.e. the change takes place over an interval of about 2-5 cm.

Unit B: traditionally known as "Escargotière", this unit corresponds to the late Iberomaurusian occupation of the site. It comprises an approximately 1.4-1.6m thickness of anthropogenic shell-rich layers with prevalent lenticular sedimentation modality. The matrix is made up of sandy silt or silty loam, but its quantity varies across lenses, so that the structure ranges from very loosely packed openwork to skeleton supported. The dominant colour is dark grey with light brown shades. Based on slight differences in sedimentological features, unit B can be divided into two subunits, B1 and B2. The lower layers (unit B1) are characterized by slightly more horizontal extension and darker greyish-brown colour than the uppermost ones (unit B2). Also, the amount of sand seems to be slightly higher in the lower part (B1), while the amount of snail shells is greater in the upper layers (B2). The content of carbonates is high to very high reaching maximum CCE values of about 81% (Fig. 3). Together with locally high contents of TOC (maximum at 9.5%), the sediments of unit B2 consist mainly of carbonates and organic matter, whereas siliceous compounds are few. Within unit B1, siliceous components increase with depth, as reflected by decreasing contents of CCE (Fig. 3), which on average are significantly lower than in B2. Ash and charcoal occur abundantly throughout units B1 and B2 as well as bone, angular centimetric limestone rubble, and heat-shattered rocks. The different sediment lenses mainly diverge in the amount/appearance of snail shells (entire and debris/burnt or fresh) as well as in ash content and are often separated by more sub-horizontal silty layers rich in ash. Part of the sand and silt consists of finely crushed snail shells. Higher ash content determines lighter grey colours, reflected in comparatively high L* values (Fig. 3). Fire activity is remarkable all through the Escargotière. Hearths are embedded within the layers and can either occur as clear combustion structures with abundant charcoalor as densely concentrated ash dumps.

The base of unit B1 displays a clear sediment boundary connected to a possible erosive disconformity. However, in some limited parts of trench V and II (west

profiles), the lower limit appears slightly more diffuse for the presence of a 10-15 cm greyreddish sandy-silt layer with snail debris and high concentrations of ash and charcoals.

Unit C: traditionally known as "Couche rouge", this unit corresponds to the early Iberomaurusian occupation of the site. The separation with overlying unit B1 is clear. The unit comprises of approximately 0.5-0.7m thick reddish-brown to yellow sand-rich sediments with minor quantities of silt and clay and variable content of limestone rubble. The structure is matrix-supported, and deposits appear moderately densely packed. The sediments are locally rich in charcoal and are dominated by sublayers of distinct colours: from dark red to yellow-white, from grey to blackishbrown. These colour variations are probably related to the variable presence of ash and to the decomposition of organic matter of various origins. In contrast to units B1 and B2, layers of unit C are characterized by lateral continuity with horizontal/sub-horizontal sedimentation mode. Since the colour, texture, grain size or composition of the sediments is relatively homogeneous, individual layers are mainly differentiated on the base of the quantity and distribution of anthropogenic contents such as charcoal, ash, lithic artefacts, and faunal remains, and based on slight variations in the sandy matrix and amount of limestone rubble. Generally, terrestrial gastropod shells are very rare (mainly crushed) or totally absent. Although there is archaeological evidence in most of the sediments, the intensity of human occupation seems to have varied. Some layers consist mainly of thin bands of sand with minor amounts of ash, while others are characterized by more evident concentrations of fire by-products with superimposed charcoal, ash micro-lenses, and various coloured shades. The lower boundary is gradual over an interval of *ca*. 5 cm.

Unit D: initial early Iberomaurusian deposit, sometimes named as "lower Couche rouge" or "Couche jaune". It is the earliest cultural unit of the site (lower part of the early Iberomaurusian deposit) and lies directly on the bedrock. Stratigraphically, it belongs to unit C, but the layers composing this unit are more homogeneous with minor quantities of limestone rubble. The unit is about 0.4-0.5m thick and consists of yellow-brown to ochre-coloured sediments made up of sandy-silt loam, densely packed, with massive structure and variable amounts of clay. Layers tend to display a subhorizontal to oblique orientation and, in contrast with unit C, layers of unit D are almost devoid of charcoal and contain few archaeological finds (Potì, 2017).

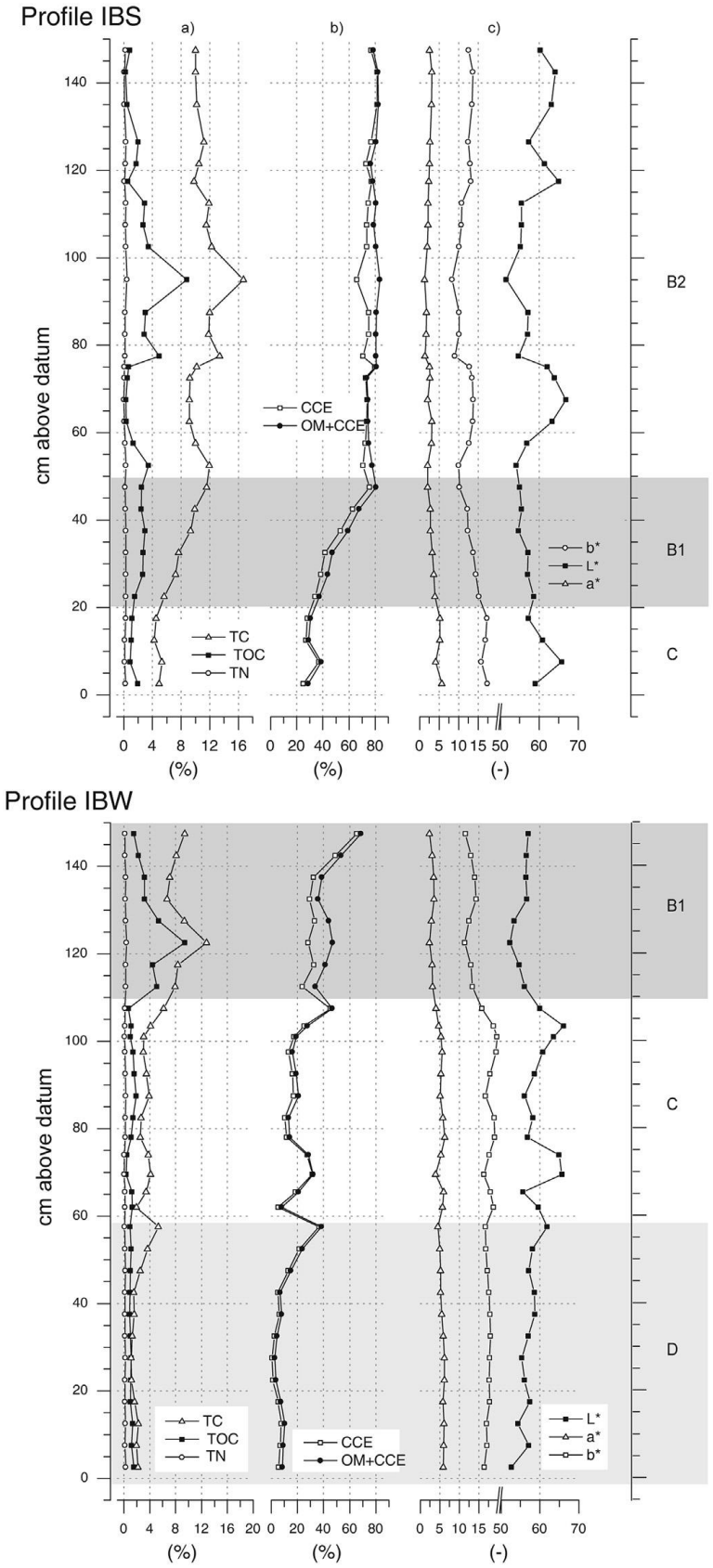

Fig. 3. Results of sedimentological measurements. a) Contents of total carbon (TC), organic carbon (TOC), and total nitrogen (TN); b) calcium carbonate equivalent (CCE) and the sum of organic matter (OM) and CCE; c) colour values in the L*a*b* colour space.

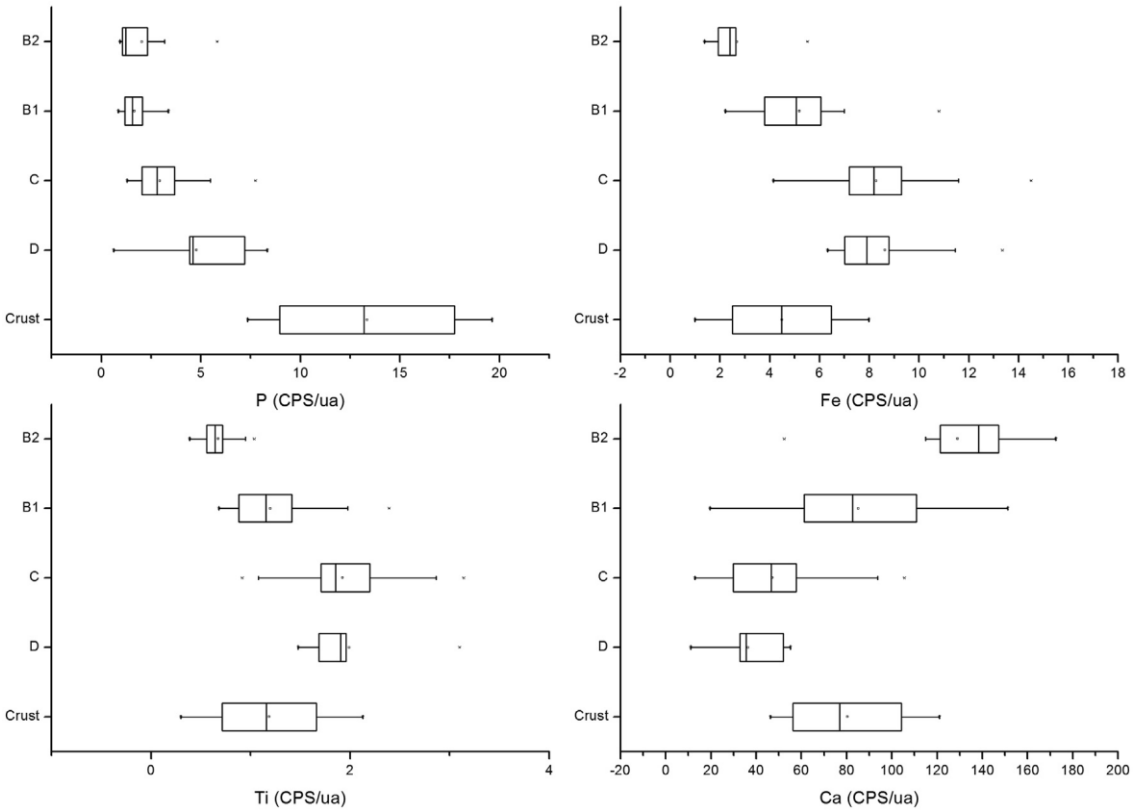

Fig. 4. Box-plots of phosphorous (P), iron (Fe), titanium (Ti) and calcium (Ca) concentrations in units B2 (n = 9), B1 (n =27), C (n =35), and D (n =12). The lowermost box-plot represents four measurements for the crust at the bottom of unit D.

During fieldwork, the boundary between units C and D was not always easy to discern due to the gradual textural change and the general homogeneity of sediment features. However, a gap in dating evidence seems to highlight the separation between the two units. The lower boundary is diffuse, with residual loam from the weathering of the bedrock limestone. At the lowermost part of unit D, the sediment is cemented to form a moderately stable crust. High concentrations of phosphorus in the groundmass (Fig. 4) and micromorphological features show that accumulation of phosphate is responsible for this encrustation. From unit B2 to unit D, average phosphorus contents increase. Iron (Fe) and titanium (Ti) show a similar behaviour, reaching maximal average values in units C and D. Calcium (Ca) behaves in an opposite pattern and attains maximal values in unit B2. While Ca reflects the high contents of carbonatic compounds in units B2 and to a lesser extent in unit B1, as indicated in high and moderately high CCE values of these layers, Fe and Ti represent non-carbonatic components. These reach maximum values in units C and D. The element patterns

suggest close similarity in geochemical signatures of units C and D. Unit B1 takes an intermediate position between units B2 and C.

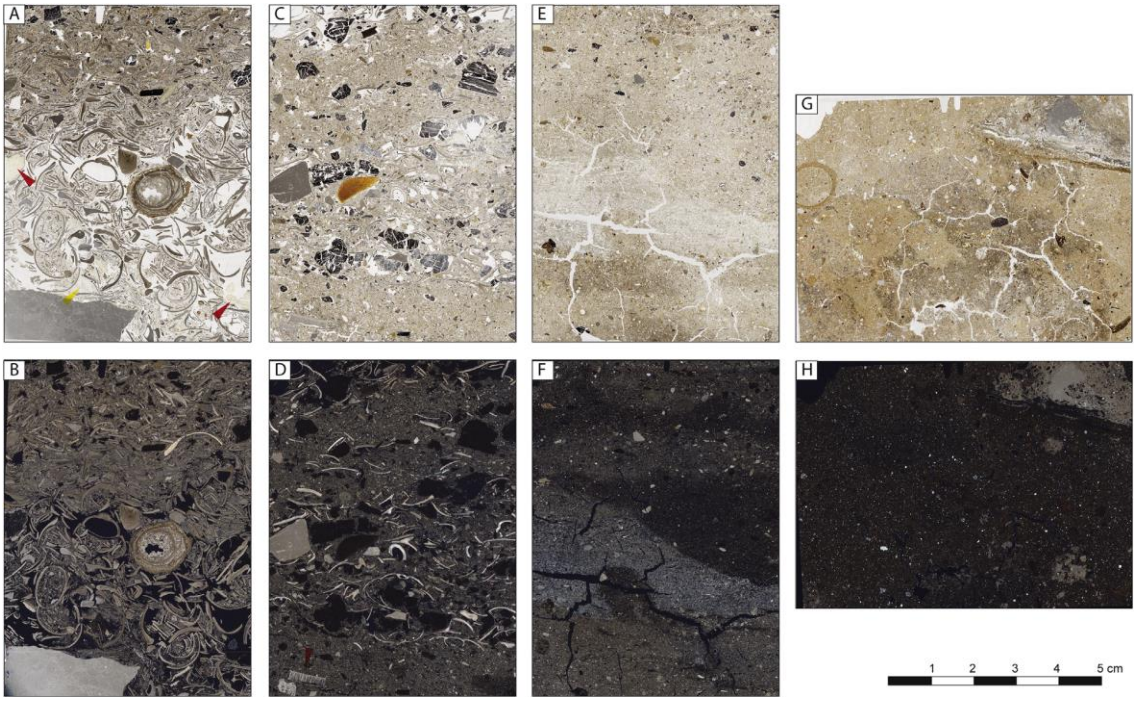

Fig. 5. Selected thin section scans from the four major chronostratigraphic units of Ifri El Baroud. (A) Snail-rich deposits of Escargotière unit B2. Loosely packed partly intact shell fragments grading into strongly compacted crushed shell towards the top. Bone fragments (red arrows), phosphate precipitates (yellow arrows) and angular limestone (bottom, thin section 302). (B) Same as A, but scanned with two perpendicular oriented pieces of polarization foil (XPL scan). Circular banded rock fragment is a small dropstone. (C) Charcoal rich sublayer of Escargotière unit B1 and transition to unit C (lowermost c. 1.5 cm). (D) Same as C, but XPL scan. Note ostrich eggshell at lower left (arrow). (E) Silty deposits of Couche rouge (unit C) with light grey phytolith-rich sublayer in the centre. Cracks are artefacts of thin section preparation (thin section 202). (F) Same as C, but XPL scan. The high birefringence of the phytolith-rich sublayer is related to presence of plant ash (see also Fig. 6 G, H). Furthermore, other layers show differences in birefringence properties, hence colour, related to porosity, organic matter, phosphate contents and frequency of opal phytoliths. (G) Silty deposits of Couche jaune (unit D). Cracks are artefacts of thin section preparation (thin section 241). (H) Same as G, but XPL scan. Dark groundmass with birefringent sand- and silt-size grains of quartz, besides local presence of secondary calcite. Note large calcium carbonate nodule with phosphate pendent at the top right. (For interpretation of the references to colour in this figure legend, the reader is referred to the Web version of this article).

5.2. Micromorphological evidence

Thin sections display general differences in sediment composition and structure between the Escargotière of units B1 and B2 on the one hand, and the Couche rouge or Couche jaune of units C and D, respectively, on the other hand, corroborating observations made in the field. The sediments of unit B2 are covered with three thin

sections taken from its lower part, whereas seven and four thin sections from profiles IBS and IBW, respectively, represent sediments from unit B1 (Fig. 2). In these Escargotière layers, the coarse material (>2mm in diameter) mainly consists of gastropod shells (Fig. 5 A, B), either crushed or preserved as entire shells. Besides these shells, few fragments of ostrich eggshell occur as well. Further components are angular fragments of mostly micritic limestone derived from roof spall, while few allochthonous rock fragments such as quartzite, flint and siltstone are present. Locally, pieces of speleothem with concentric arrangements of calcite crystals are found (Fig. 5 A, B). Fragments of well-preserved charcoal, up to 20mm in length, are the most common component of the organic remains (Fig. 5 C, D), while few large pieces of fresh plant remains, mostly wood, occur as well (Fig. 6 A). Bone is present in low amounts and mostly as small fragments (<10 mm). Locally, herbivorous coprolites (dung) are found (Fig. 6 B), which contain phytolith-rich plant fragments and heavily dissolved calcium oxalate druses (Fig. 6 C, D). The small amount of fines (~5-2000 µm) mainly consists of shell fragments, ash calcite, fine charcoal and very few quartz and other siliceous sand grains. In addition, pieces of amorphous organic matter are found in this size class. Locally, opal phytoliths occur in comparatively low numbers. The so-called micromass (submicroscopic particles ~< 5 µm in diameter) is light yellowish-brown to grey, probably composed of organic matter and finely dispersed calcite. The birefringence fabric is calcitic crystallitic.

The thin sections from units B2 and B1 show three different sediment facies. The first facies are loosely packed deposits of mostly intact shells (Fig. 5 A, lower) with few other components including bone and limestone fragments, but almost no charcoal. In many cases, the interior pores within the shells are empty but occasionally they contain isotropic clusters of phosphate, possibly representing remains of mollusc bodies. In addition, infillings of phosphate (Fig. 6 E) and organic matter, with layered internal structures resembling dung are found in between different shells. The origin of this dung is unclear. This facies probably represents dumps of intact shells placed at a certain spot after consumption of the mollusc. The second facies is represented by heavily compacted deposits of crushed shell mixed with other components. It appears that layers of this facies represent mixed deposits of rake-out sediment near fireplaces, which were later compacted by trampling. The effect of trampling on one of the shell dumps is nicely preserved in thin sections 302 (Fig. 5 A, B) and 303, which display a

transition from intact snail shells to completely crushed shells topped by heterogeneous deposits of the second facies. The third facies type is characterized by presence of comparatively few large shell fragments and high amounts of other components including limestone fragments, charcoal, bone and siliceous or carbonatic fines. This facies represents a transition towards the underlying sediments of the Couche rouge, as clearly indicated in the lowermost part of unit B1 in profile IBS. Boundaries between these sublayers are often clear due to sudden changes in the composition of coarse materials. The high degree of compaction of most sublayers and missing evidence for post-depositional bioturbation across sublayers testify to little mechanical disturbance after deposition and trampling. Furthermore, signs of post-depositional biochemical changes such as precipitation of secondary carbonates are very limited, hence the micromorphological observation indicates excellent preservation of the primary stratification corroborating field evidence.

The Couche rouge deposits of unit C are represented in three and six thin sections from profiles IBS and IBW, respectively, while unit D (or Couche jaune) is covered by six thin sections from profile IBW (Fig. 2). These sediments contain few to very few coarse particles mostly consisting of crushed gastropod shells, pieces of angular limestone, and charcoal. The layers are comparatively rich in fines consisting of sand and silt grains of quartz and other siliceous minerals (Fig. 5E-H). In some layers increased amounts of carbonates composed of limestone rock fragments and clusters of ash calcite occur in the sand fraction. Locally, high amounts of small (<2 mm) plant fragments are found (Fig. 6 F), rarely preserved as organic tissue, but mostly as articulated (or anatomically connected) phytoliths of different shapes including multicellular lattices and elongated forms. Single cell phytoliths are rare, but also more difficult to identify. In comparison with layers of the Escargotière, phytoliths are more numerous in the Couche rouge deposits and are often responsible for the black colour of the groundmass under crossed polarized light. The micromass is yellowish brown to light grey and the b-fabric mostly undifferentiated. In case of ash-rich layers, a crystallitic b-fabric is observed.

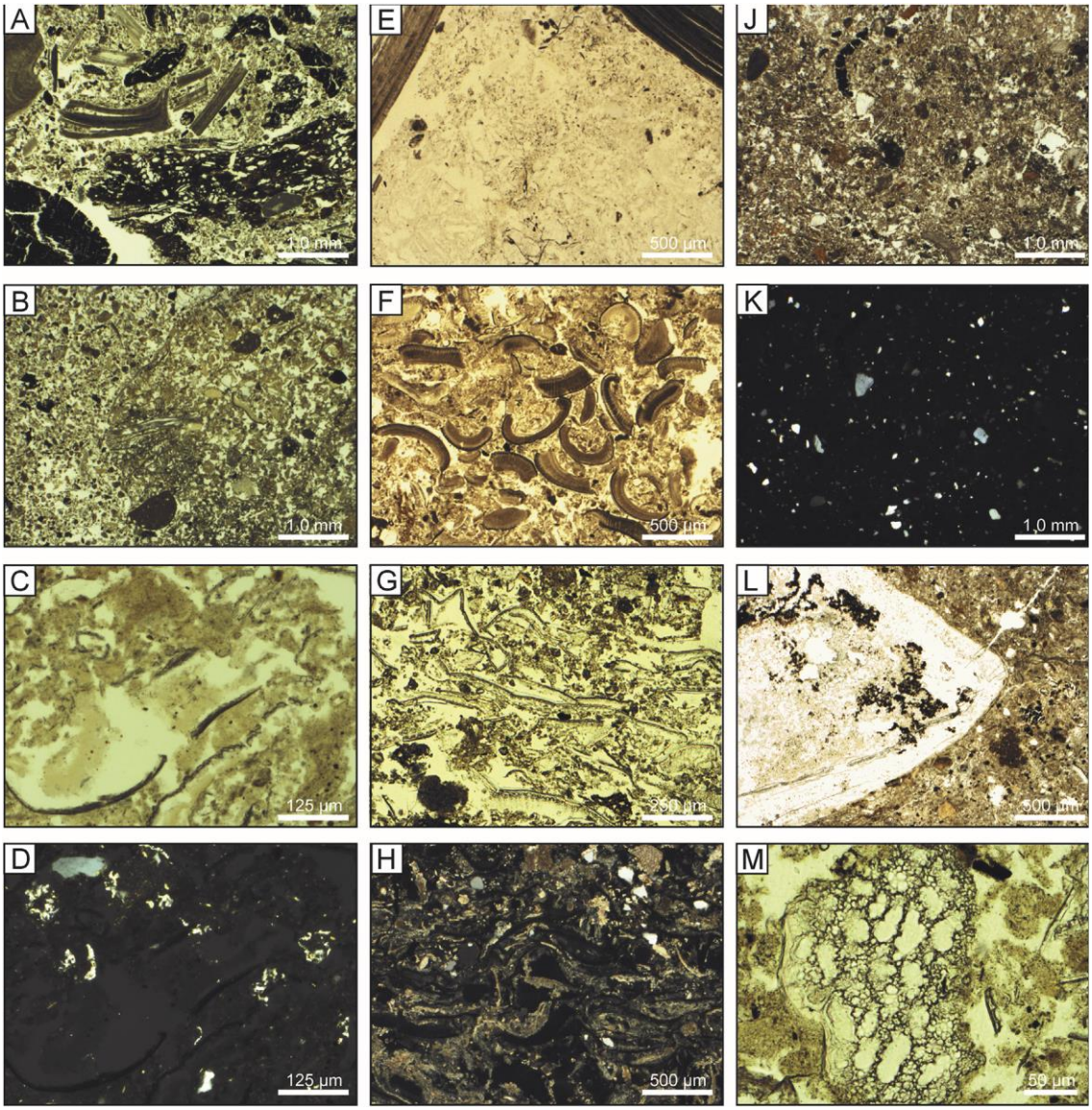

Fig. 6. Micrographs of selected thin sections from Ifri El Baroud. (A) Charcoal, mollusc shell and piece of fresh wood in unit B1 (ts 193, PPL). (B) Groundmass (left) and herbivorous dung (middle and right) in unit B1. The dung consists of plant fragments, amorphous organic material, phosphate, and few mineral grains (ts 193, PPL). (C) Detail of dung pellet of Fig. 6 B, showing plant fragments with articulated phytoliths, and phosphate precipitates (ts 193, PPL). (D) Same as Fig. 6 B but captured under crossed polarizers (XPL). Note the presence of partly dissolved calcium oxalate druses (ts 193). (E) Infillings of phosphate between shell fragments of unit B2 (ts 302, PPL). (F) Concentration of plant fragments probably derived from grass culms in unit C. The outer surfaces of the fragments are bordered by articulated phytoliths (ts 323, PPL). (G) Elongated articulated phytoliths in subhorizontal orientation in the ash layer of unit C (ts 202, PPL). (H) Birefringent ash particles in between phytoliths (black) from the same layer as Fig. 6 G (ts 202, XPL). (J) Groundmass of unit D with plenty of sand- and silt-sized mineral grains of quartz and feldspar besides organic materials and charcoal (ts 242, PPL). (K) Same as Fig. 6 J but captured under XPL. Note dark colour of groundmass, related to presence of isotropic materials including organic matter and phosphates. Birefringence is caused by mineral grains of quartz and few feldspar (ts 242). (L) Carnivore coprolite in the phosphate cemented crust of unit D (ts 417, PPL). (M) Thermally altered phytolith showing partial melting of opal and formation of vesicular pores (ts 231, unit D). (For interpretation of the references to colour in this figure legend, the reader is referred to the Web version of this article.)

Thin sections from unit C mostly display a stacked sequence of thin (<5 cm) continuous or wedging-out sublayers of different sedimentary composition, separated from each other by horizontal or moderately inclined upper and lower boundaries (Fig. 5 E, F). In the upper 3 cm of thin section 211, almost vertically running interfaces between materials of different sedimentary compositions indicate mechanical disturbance, possibly due to trampling, but the primary layering of the sediments is still preserved. A moderate post-depositional enrichment with phosphate is indicated by isotropic rims on limestone fragments and infillings of phosphate in horizontal pores. Furthermore, the dark colour of the groundmass, when inspected under crossed polarizers, points to diffuse phosphate enrichment in some sublayers. Secondary carbonatesmainly occur as orthic or, much more rarely, disorthic calcite nodules. One of the most interesting layers of unit C is included in thin section 202 (Fig. 5 E, F). It is about 3 cm thick and consists of ashed plant material, clearly showing a sub-horizontal orientation of the elongated siliceous remains (Fig. 6 G, H). Since charcoal is absent and the layer is preserved in a considerable lateral extent, it appears likely that the burned matter originates from grasses which were used to cover the cave floor and were intentionally burned. Horizontal concentrations of plant fragments and articulated phytoliths have been microscopically documented in several sublevels of units C and D, indicating the repeated intentional use of grasses as floor coverings during the early Iberomaurusian.

Thin sections from unit D show a quite homogenous composition of these yellowish-brown deposits getting more patchy in colour towards the bottom of the sequence (Fig. 5 G and H). The groundmass is composed of sand-to silt sized grains of quartz and silicates, organic matter and charcoal (Fig. 6 J, K). Phosphate enrichment is indicated by diffuse impregnation of the groundmass and formation of phosphate crusts in the lowermost part. Part of the phosphate originates from carnivore and herbivore coprolites (Fig. 6 L), of which many fragments are found with a tendency to increasing numbers toward the bottom. Additionally, calcitic nodules testify the local accumulation of secondary carbonates. Similar to deposits of unit C, partial melting of opal by burning has caused irregular cell structures of phytoliths (Fig. 6 M). Large numbers of plant remains and phytoliths are also present in the phosphate cemented lowermost part of unit D.

5.3. Chronological framework

Table 1 shows the twenty-five new AMS radiocarbon dates and their correlation with spits, layers and units (Fig. 2), while Table 2 shows the published suite of radiocarbon dates from the site (Görsdorf and Eiwanger, 1999). Both uncalibrated and calibrated dates are shown.

The new dates confirm the general cultural pattern detected by the previous radiocarbon ages, strengthening the understanding of the Late Glacial and early Holocene developments in the northeastern region of Morocco. Altogether, four main sets of ages can be distinguished (Fig. 7). They show clear correlation with the major cultural and stratigraphic divisions recognized at the site. The younger group of dates comes from the base on unit A of trench III and IV and confirms its attribution to a phase between the final Younger Dryas and the Preboreal with ages ranging roughly between 11 and 9 ka cal BP. One date (KIA 511-I) additionally corroborates the presence of sub-recent disturbances, as already highlighted by stratigraphic observations. The second group of dates comes from the shell-rich layers of unit B of trenches II, III, IV and V and covers the interval between 15.5 and 12.9 ka cal BP. Chronologically, unit B corresponds to a palimpsest of occupations occurred during GI-1 (Rasmussen et al., 2014). The third group is from the finely laminated layers of unit C (trenches II, IV and V) which have provided a set of dates ranging between 19.4 and 16 ka cal BP, while the oldest group is represented by samples of layers of unit D (only from trench V), showing a distribution between 22.7 and 20 ka cal BP. The dates from unit C and D confirm that the early Iberomaurusian occupations occurred during Greenland Stadial (GS) 2.1 a-b-c (Rasmussen et al., 2014), delimited by Heinrich events 2 and 1 (HE phases acc. to Fletcher and Sánchez-Goñi, 2008) (Fig. 7 A).

Radiocarbon dates show a general pattern of increasing age with depth. Few inversions of age within layers of unit B (Escargotière) could be due to the movements of charcoal through the loose openwork snail lenses. In contrast, the presence among the dates from the early part of the sequence - within trench V layers w-52 and w-51 of unit D - of a younger determination (COL3778.1.1) does not have a clear explanation. It could be due either to contamination of sediments during flotation (that resulted in the incorporation of younger charcoal) or to the fall of carbon from the upper Escargotière profiles which was then inadvertently sampled during excavation. Post-depositional

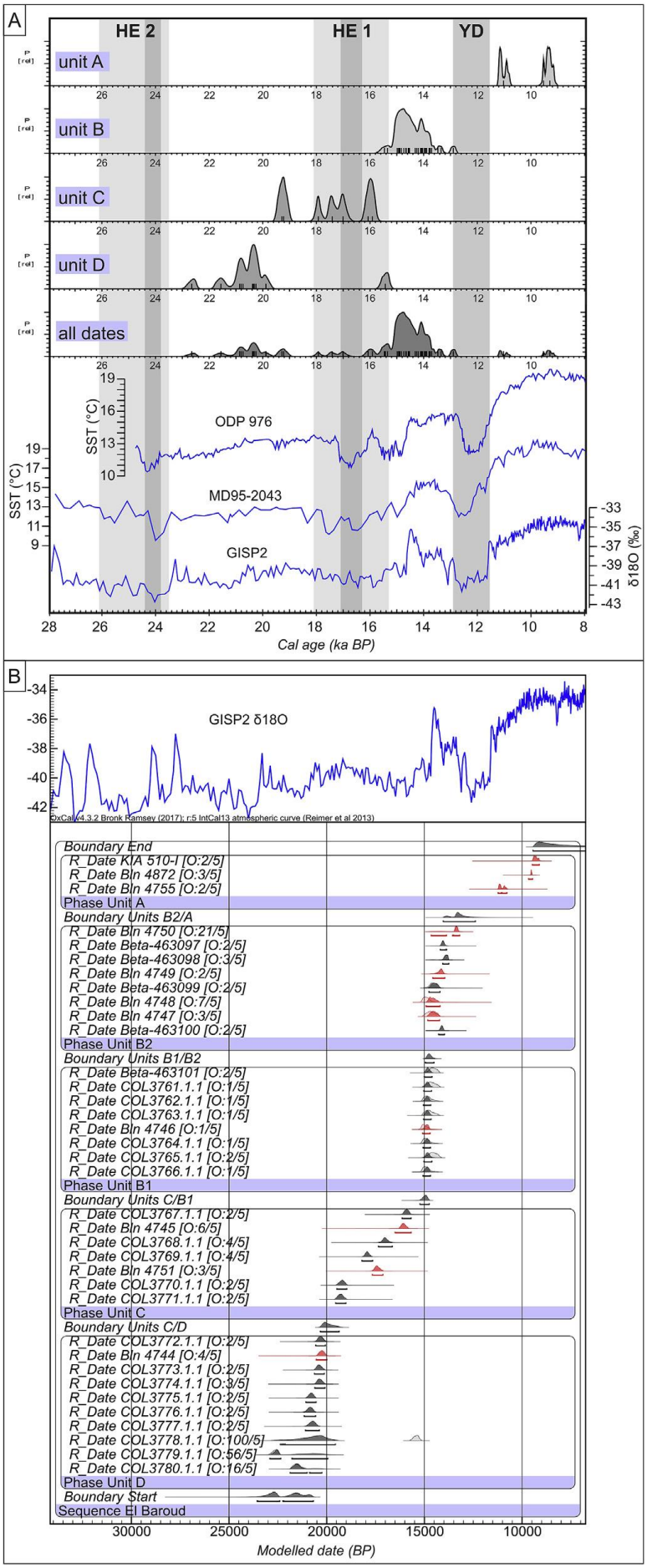
A
HE 2
HE 1
YD
unit A
unit B
unit C
unit D
all dates
ODP 976
MD95-2043
GISP2
SST (°C)
δ18O (‰)
Cal age (ka BP)
B
GISP2 δ18O
Boundary End
R_Date KIA 510-I [O:2/5]
R_Date Bln 4872 [O:3/5]
R_Date Bln 4755 [O:2/5]
Phase Unit A
Boundary Units B2/A
R_Date Bln 4750 [O:21/5]
R_Date Beta-463097 [O:2/5]
R_Date Beta-463098 [O:3/5]
R_Date Bln 4749 [O:2/5]
R_Date Beta-463099 [O:2/5]
R_Date Bln 4748 [O:7/5]
R_Date Bln 4747 [O:3/5]
R_Date Beta-463100 [O:2/5]
Phase Unit B2
Boundary Units B1/B2
R_Date Beta-463101 [O:2/5]
R_Date COL3761.1.1 [O:1/5]
R_Date COL3762.1.1 [O:1/5]
R_Date COL3763.1.1 [O:1/5]
R_Date Bln 4746 [O:1/5]
R_Date COL3764.1.1 [O:1/5]
R_Date COL3765.1.1 [O:2/5]
R_Date COL3766.1.1 [O:1/5]
Phase Unit B1
Boundary Units C/B1
R_Date COL3767.1.1 [O:2/5]
R_Date Bln 4745 [O:6/5]
R_Date COL3768.1.1 [O:4/5]
R_Date COL3769.1.1 [O:4/5]
R_Date Bln 4751 [O:3/5]
R_Date COL3770.1.1 [O:2/5]
R_Date COL3771.1.1 [O:2/5]
Phase Unit C
Boundary Units C/D
R_Date COL3772.1.1 [O:2/5]
R_Date Bln 4744 [O:4/5]
R_Date COL3773.1.1 [O:2/5]
R_Date COL3774.1.1 [O:3/5]
R_Date COL3775.1.1 [O:2/5]
R_Date COL3776.1.1 [O:2/5]
R_Date COL3777.1.1 [O:2/5]
R_Date COL3778.1.1 [O:100/5]
R_Date COL3779.1.1 [O:56/5]
R_Date COL3780.1.1 [O:16/5]
Phase Unit D
Boundary Start
Sequence El Baroud
Modelled date (BP)

Fig. 7. A) Cumulative probability distributions of calibrated radiocarbon dates from Ifri El Baroud divided per stratigraphic units. Both new and old dates are included (Görsdorf and Eiwanger, 1999). Environmental proxies: curves display changes in sea surface temperature of the Mediterranean as detected from marine cores MD95-2043 (Cacho et al., 2001) and ODP 976 (Martrat et al., 2014), Alboran Sea. The lower curve shows the d18O record of GISP2 ice core, Greenland (Grootes et al., 1993). Grey bars display the early, main and late phases of Heinrich events 2 and 1 as recognized in thepollen record of the marine core MD95-2043 (Fletcher and Sánchez-Goñi, 2008), which is located at about 160 km NNE of Ifri El Baroud. The grey bar of the Younger Dryas has been drawn according to the recent compilation of d 18O and Ca2þ records of Greenland ice cores (Rasmussen et al., 2014). B) Bayesian plot showing the radiocarbon dates (calibrated and modelled) relating to trench II and trench V excavation (for units D-C-B1-B2) and to trench II and IV excavation (for unit A). Dates from the 1995 and 1996 field excavations are shown in red. The plot delivers probability density functions for the start and end of the different occupation phases. The sequence is compared to the GISP2 d18O record, Greenland (Grootes et al., 1993).

alterations are excluded because layers of unit D did not showany evidence of disturbance and dates below and above this younger determination appear in clear order.

The Bayesian plot (Fig. 7 B) delivers probability distributions for the start/end boundaries of the units representing the transition between successive phases. The model exhibits strong correlation between age and sample origin. However, according to the modelling, there is a high probability that samples COL3778.1.1 and COL3779.1.1 from unit D are statistical outliers. Concerning COL3778.1.1, this was already clear on technical grounds (see above). Concerning samples COL3779.1.1 and its relationship with sample COL3780.1.1, it is worth mentioning that the two samples come from the same layer. Although sample COL3779.1.1 was retrieved from a higher position (in terms of absolute altitude) than sample COL3780.1.1, the stratigraphic relationship between the two samples is hard to assess because they come from the sediment of two different sub-squares (not adjacent) separated by the emerging bedrock.

B) Bayesian plot showing the radiocarbon dates (calibrated and modelled) relating to trench II and trench V excavation (for units DC- B1-B2) and to trench II and IV excavation (for unit A). Dates from the 1995 and 1996 field excavations are shown in red. The plot delivers probability density functions for the start and end of the different occupation phases. The sequence is compared to the GISP2 d18O record, Greenland (Grootes et al., 1993).

Lab no.	Sample ID	Trench	Position	Unit	Charcoalspecies	14C-age (yr BP Uncalibrated)	δ13C (‰)	Cal-age (yrcal BP, 95.4%)

Beta - 463097	IB15Pos 48	V	G17b_spit. 5	B2	*Juniperus/Te traclinis*	12160±40	-20	14160-13920
Beta - 463098	IB15Pos 119	V	G17b_spit. 10	B2	*Juniperus/Te traclinis*	12040±40	-20,9	14050-13730
Beta - 463099	IB15Pos 432	V	G17b_spit. 15	B2	Leguminosae	12430±40	-23,1	14870-14190
Beta - 463100	IB15Pos 514	V	G17b_spit. 20	B2	Leguminosae	12220±40	-21,1	14230-13990
Beta - 463101	IB15Pos 914	V	G17b_spit. 25	B1	Leguminosae	12440±40	-22,4	14890-14210
COL376 1.1.1	IB15Pos 953	V	G17a_spit. 27	B1	Leguminosae	12477±58	-24,4	15090-14210
COL376 2.1.1	IB15Pos 974	V	G17a_spit. 28	B1	Leguminosae	12547±60	-26,0	15190-14470
COL376 3.1.1	IB15Pos 1005	V	G17a_spit. 29	B1	*Vicia*	12514±62	-20,9	15160-14320
COL376 4.1.1	IB15Pos 1014	V	G17a_spit. 30	B1	Leguminosae	12577±63	-24,0	15200-14600
COL376 5.1.1	IB15Pos 1033	V	G17a_spit. 31	B1	Leguminosae	12444±62	-23,1	14990-14150
COL376 6.1.1	IB15Pos 1054	V	G17a_spit. 32	B1	Leguminosae	12582±63	-23,0	15210-14610
COL376 7.1.1	IB15Pos 1075	V	G17a_spit. 33	C	Leguminosae	13235±62	-22,0	16110-15710
COL376 8.1.1	IB15Pos 1095	V	G17a_spit. 34	C	Leguminosae	14005±67	-23,4	17250-16770
COL376 9.1.1	IB15Pos 1115	V	G17a_spit. 35	C	Leguminosae	14732±72	-20,9	18130-17730
COL377 0.1.1	IB15Pos 1158	V	G17b_spit. 37	C	Leguminosae	15932±76	-21,2	19500-18940
COL377 1.1.1	IB15Pos 1171	V	G17b_spit. 38	C	Leguminosae	15985±81	-22,0	19570-19010
COL377 2.1.1	IB15Pos 1197	V	G17b_spit. 40	D	Leguminosae	16837±81	-21,6	20580-20060
COL377 3.1.1	IB15Pos 1210	V	G17b_spit. 41	D	Leguminosae	16902±83	-23,2	20640-20120
COL377 4.1.1	IB15Pos 1237	V	G17b_spit. 43	D	Leguminosae	16878±81	-22,1	20620-20100
COL377 5.1.1	IB15Pos 1263	V	G17b_spit. 45	D	*Juniperus/Te traclinis*	17249±80	-19,9	21070-20550
COL377 6.1.1	IB15Pos 1276	V	G17b_spit. 46	D	Leguminosae	17296±87	-20,2	21140-20580
COL377 7.1.1	IB15Pos 1289	V	G17b_spit. 47	D	*Quercus*sp. evergreen	17183±123	-39,0	21080-20400

COL3778.1.1	IB15Pos1315	V	G17b_spit.49	D	*Juniperus/Tetraclinis*	12907±65	-20,3	15690-15170
COL3779.1.1	IB15Pos1341	V	G17b_spit.51	D	*Juniperus/Tetraclinis*	18768±103	-20,3	22930-22370
COL3780.1.1	IB15Pos1374	V	F17d_spit.53	D	*Juniperus/Tetraclinis*	17798±91	-19,4	21880-21240

Table 1. New set of 14C ages from Ifri El Baroud trench V. The calibration of 14C dates was calculated using CalPal software (Weninger and Joris, 2008) and Intcal13 calibration curve (Reimer et al., 2013).

Lab no.	**Sample ID**	**Trench**	**Position**	**Unit**	**Charcoalspecies**	**14C-age (yr BP Uncalibrated)**	**δ13C (‰)**	**Cal-age (yrcal BP, 95.4%)**
KIA 511-I	IB 96-Pr.D	IV	H11_spit.3	A	nd	1650±40	-21,92	1670-1430
KIA 510-I	IB96-Pr.C	IV	I11_spit.3	A	nd	8300±60	-22,85	9510-9070
Bln 4872	IB96-M (IB96-Bnr.97)	IV	K11?_spit.3	A	nd	8556±52	-22,29	9590-9470
Bln 4755	IB95-S	III	E11_spit.6	A	nd	9677±60	-22,42	11320-10720
Bln 4926	IB96-H (IB96-4)	IV	I11_spit.6	B	nd	11027±49	-22,43	13050-12730
Bln 4750	IB95-L	II	C/D 17-18_spit.2	B	nd	11508±60	-22,4	13470-13230
Bln 4871	IB96-I (IB96-Anr.41)	IV	H11?_spit.5	B	nd	11639±58	-22,92	13590-13350
Bln 4754	IB95-R	III	E10_spit.8	B	nd	11895±64	-22,76	13860-13540
Bln 4928	IB96-F (IB96-21)	IV	I13_spit.15	B	nd	11926±68	-22,61	13980-13540
Bln 4933	IB96-E (IB96-94)	IV	I11_spit.16	B	nd	11946±52		13980-13620
Bln 4931	IB96-G (IB96-51)	IV	I11_spit.10	B	nd	12083±61	-21,92	14130-13730
Bln 4752	IB95-P	III	E10_spit.13	B	nd	12128±70		14200-13760
Bln 4929	IB96-D (IB96-38)	IV	I15_spit.17	B	nd	12172±61	-22,78	14220-13860
Bln 4753	IB95-Q	III	E10_spit.10	B	nd	12198±65	-22,23	14270-13910

Bln 4749	IB95-H	II	C/D 17_spit.7	B	nd	12253±67	-22,49	14440-13960
Bln 4927	IB96-L (IB96-5)	IV	K11_spit.14	B	nd	12294±49	-22,65	14500-14020
Bln 4934	IB96-96	IV	L15-16-17_spit.17/18	B	nd	12309±58	-22,59	14630-13990
Bln 4747	IB95-E	II	C17 [bef.7-8]_spit.13	B	nd	12481±57	-23,05	15100-14220
Bln 4748	IB95-F	II	D17_spit.9	B	nd	12574±65	-23,07	15210-14570
Bln 4932	IB96-C (IB96-83)	IV	H15_spit.25	B	nd	12607±75		15250-14610
Bln 4746	IB95-D	II	D/E 17_spit.16	B	nd	12626±59	-23,09	15240-14720
Bln 4930	IB96-N (IB96-49)	IV	K17_spit.29	B	nd	12841±80		15630-15070
Bln 4873	IB96-B (IB96-Cnr.88)	IV	H16?_spit.30-31	B	nd	12932±78		15740-15180
Bln 4745	IB95-C	II	C18_spit.19	C	nd	13359±72	-22,6	16290-15850
Bln 4751	IB95-M	II	F17-18_spit.22	C	nd	14299±72		17650-17170
Bln 4911	IB96-A (IB96-68)	IV	I17_spit.35	D	nd	16485±68	-21,89	20120-19640
Bln 4744	IB95-A	II	E17-18_spit.24	D	nd	16777±83	-22,09	20510-19990

Table 2. 14_C ages from Ifri El Baroud (after Görsdorf and Eiwanger, 1999). The calibration of 14C dates was calculated using CalPal software (Weninger and Joris, 2008) and Intcal13calibration curve (Reimer et al., 2013).

5.4. Anthracological data

Within the analysed samples, a total of 8281 wood charcoal fragments were identified corresponding to a minimum of 12 taxa. Despite the great temporal extension studied and the chronological resolution of the sequence, the anthracological data show a certain continuity in the local woody vegetation throughout the sequence. This seems to indicate a great continuity in plant fuel supply strategies throughout the

Iberomaurusian (Fig. 8). Thus, the local landscape would be characterized by the presence of the plant formations of *Juniperus/Tetraclinis* (savin or araar) together with woody legume taxa (Fabaceae) and low percentages of other taxa such as Labiatae, *Ephedra* sp., *Fraxinus sp.*, *Rhamnus-Phillyrea*, Maloideae, *Salix-Populus*, Compositae and *Quercus* sp. evergreen (Carrión Marco et al., 2018). The homogeneous anatomical structure of Juniperus and Tetraclinis does not allowthe discrimination of these genera, nor the species of juniper gathered, being able to be the most thermophilous species (J. *oxycedrus, J. phoenicea*) or the cryophilous ones (*J. communis, J. thurifera, J. sabina*), whose presentday range covers from thermo-Mediterranean to supra- Mediterranean belts under dry or semiarid bioclimatic conditions (Costa et al., 2005). Junipers form open heliophilous forests in which sunlight reaches the ground abundantly, allowing the development of shrub species with similar ecological requirements (Charco, 1999).

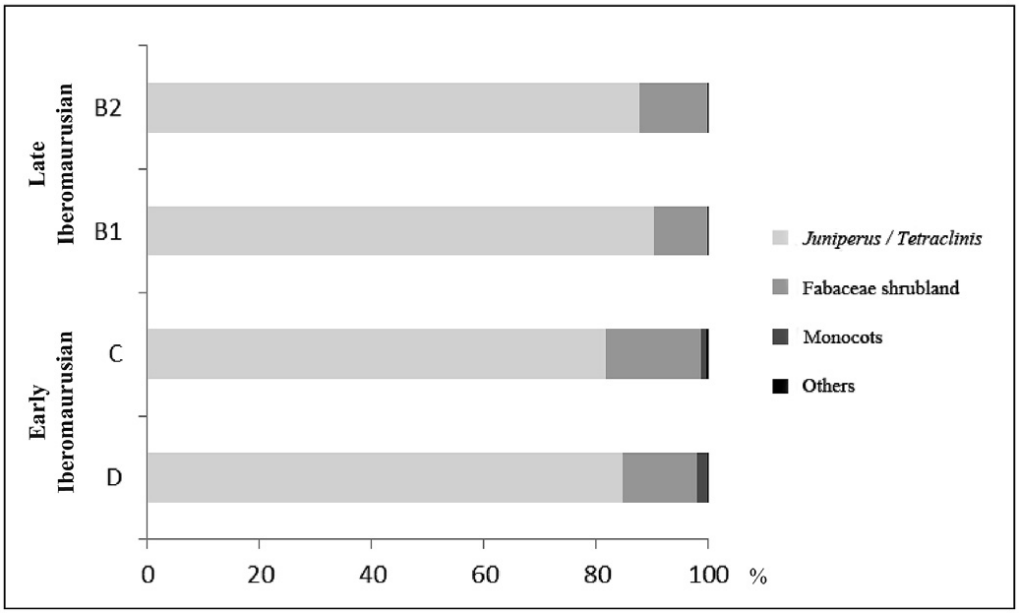

Fig. 8. Anthracological data from the sequence of Ifri El Baroud.

5.5. Seed and fruit remains

Preliminary evidence for the use of plants has been verified throughout the full sequence of Ifri El Baroud by the ongoing analyses of seeds and fruits. The examination of 376 samples has provided a rich assemblage of well-preserved carbonised plants that could have been collected for different purposes, such as food and basketry. The data recorded for the time being indicate a certain difference between the species recorded in early and late Iberomaurusian levels. In the early Iberomaurusian levels (units C and D),

seeds of *Juniperus*, Lamiaceae and wild legumes are documented. In late Iberomaurusian layers (unit B), the number of plants remains increase considerably, and the most common remains belong to the tribe Fabeae, which includes seeds of the genera *Vicia*, *Lathyrus* and *Lens*. In addition, rhizome fragments of Alfa grass (*Stipa tenacissima*) have been recorded in both early and late Iberomaurusian layers.

5.6. Palynological data

An overall good state of preservation of pollen grains was found in the analysed sediment samples. Pollen percentages are given in Fig. 9. In order to carry out a detailed vegetation reconstruction, pollen samples have been sorted according to their estimated chronology including both profiles.

The early Iberomaurusian levels (units D and C) are characterized by high percentages of herbs (58.5-67.2% unit C and 68.2-77.8% unit D). The herbaceous pollen assemblage is dominated by Poaceae (29.3-45.2%), *Artemisia* (7.7-17.4%), *Ephedra fragilis* type (3.3-8.6%), *Helianthemum* type (2.9-10.4%), Resedaceae (3.1-7.1%) and Chenopodiaceae (8.7-18.2%) reflecting arid and cold climatic conditions corresponding to the GS-2.1. The percentages of trees (<13%) and shrubs (<30%) are reduced, being especially significant the absence of some thermophilous elements that are documented in the upper units. In any case, the documentation of a continuous curve of *Juniperus/Tetraclinis* type, whose values (2.5-4.5%), like those of evergreen *Quercus* (3.3-5.6%), *Phillyrea*, *Pistacia lentiscus* and *Rhamnus alaternus* type, increase slightly in unit C, is noteworthy. This demonstrates the existence of refuge areas for the most thermophilic flora in areas near the coast even in periods of climatic detriment such as those of the aforementioned GS-2.1 Stadial.

Unlike the previous ones, the late Iberomaurusian levels (units B1 and B2) show a general decrease in herbaceous pollen (5.5-13.4%), and a large increase in the percentages of trees (37.2-53.1%) and shrubs (39.6-50.5%). The arboreal pollen assemblage is dominated by evergreen *Quercus* (14.4-24.1%) and *Juniperus/Tetraclinis* type (6.3-13.8%), indicating the establishment of evergreen sclerophyllous oak (holm and/or kermes oak, *Quercus ilex* or *Q. coccifera*) woodlands in the surroundings of the site (López-Sáez et al., 2010). Other elements such as *Abies* (<5%), *Acer* (<3%), Cedrus (2.5e5.9%), deciduous *Quercus* (3.2-7.5%), *Pinus pinaster* (2-6.5%) and *P. halepensis/pinea* type (3-10%) have probably a regional or extra-regional origin (Alba-

Sánchez et al., 2018; López-Sáez et al., 2015), while *Salix* (2-7%) and *Fraxinus* (2-5%) arepart of the riparian forests. The shrub vegetation shows a remarkable importance, with a good representation of the xerothermophilous macchia mainly composed of *Pistacia lentiscus* (2.3-6.9%), *Genista* type (3.1-10.9%) and *Phillyrea* (2.8-6.6%), as well as *Erica arborea* type, *Cistus ladanifer* type, Myrtus communis and Rhamnus alaternus type. *Crataegus* type is also represented, while other pollen taxa representing Ibero-African elements (*Periploca*, *Whitania*, *Ziziphus*) are also present sporadically (<4%). Among the herbs, only Poaceae (3.3-11.2%) show noticeable values. Anthropogenic types (*Aster*, Cardueae, Cichorioideae), excluded from the pollen sum, are also present in relatively high percentages, indicating their indirect contribution to the sediments by humans during the late Iberomaurusian occupation (units B1 and B2) of the cave (López- Sáez et al., 2003, 2006).

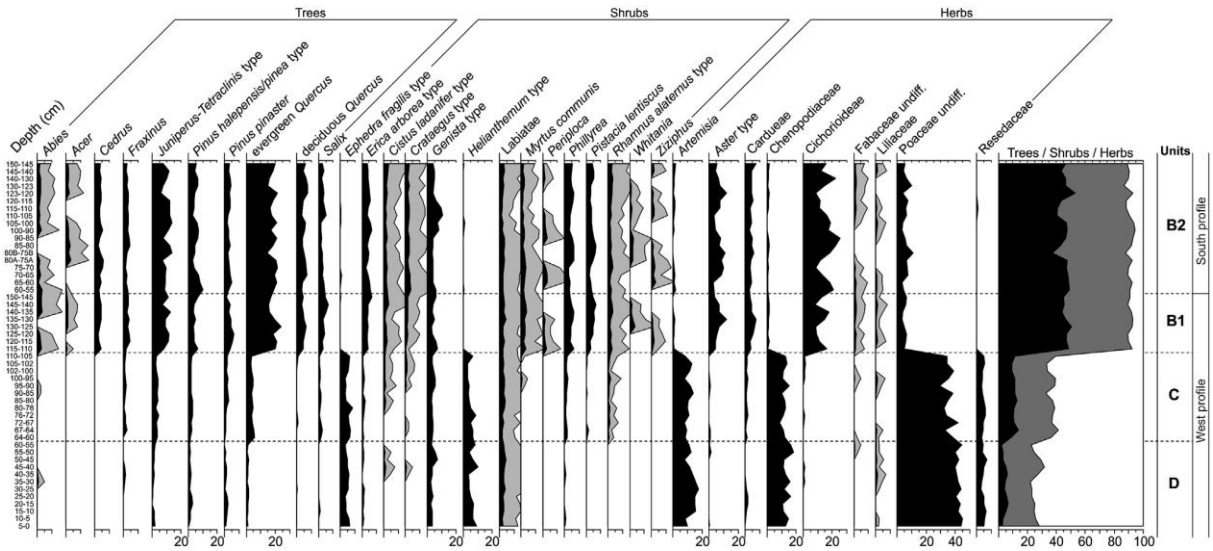

Fig. 9. Palynological diagram from Ifri El Baroud. Exaggeration curves are 5%.

5.7. Phytolith assemblages

Phytoliths were abundant in all samples throughout the Iberomaurusian deposit (from 0.4 to 3.1 million phytoliths per gram of sediment, Table 3). Most of the phytolith assemblages derived from monocotyledonous plants and particularly from the Pooideae grass subfamily. Phytoliths from woody/herbaceous dicotyledons were also common in all samples, with an average close to 34% (Fig. 10). This is especially noteworthy given that dicotyledonous plants are minor phytolith producers. Moreover, silica aggregates which are commonly produced by woody plants were observed in most of the samples,

in association to other calcitic microfossils, including ash pseudomorphs-calcite pseudomorphs after calcium oxalate crystals' heating to at least 450 ºC, primarily originating from wood and dicotyledonous leaves (Fig. 11a). These displayed morphologies are directly comparable to Juniperus, which are consistent with the macrobotanical and palynological records (Brochier and Thinon, 2003; Portillo et al., 2017a; Wattez and Courty, 1987). Also of significance is the presence of phytoliths showing evidence for partial melting, resulting in deformations and bubbling due to high temperatures (ca. 800 ºC, Canti, 2003). In addition, other silica biogenic components such as diatoms were observed in many phytolith slides, also indicative of humid conditions.

Phytolith assemblages vary across the occupational sequences and even within single layers. The transition between the early Iberomaurusian units D and C displays a general increase of grasses. The uppermost layer of unit D shows relatively large proportions of grass inflorescence phytoliths (up to 28%, Fig. 10). The presence of phytoliths from their floral parts may indicate a selection of these plant materials and could potentially constitute a seasonality indicator (spring-autumn). In both profiles IBS and IBW, the upper layers of unit C show overwhelmingly high concentrations of multicellular epidermal jigsaw puzzle-shaped phytoliths produced by dicotyledonous leaves (Fig. 11f), which are readily available in humid wetland environments (Bozarth, 1992; Geis, 1973; Tsartsidou et al., 2007). These phytolith-rich assemblages are also composed of articulated structures from the leaves and culms of grasses. Further, the relatively high proportions of anatomically connected phytoliths suggest that these have not been reworked, as multicellular forms are fragile to mechanical degradation (Jenkins, 2009; Portillo et al., 2017b; Shillito, 2011), as observed through thin-section micromorphology. Diagnostic phytoliths from the leaves of the Arecaceae family (palms) and Cyperaceae (sedges) are also present within the early occupation (units C and D), while they are almost absent in the lower Escargotière (unit B1) and not represented in the upper part of the late Iberomaurusian sequence (upper B2), where the phytolith record is dominated again by grasses (Fig. 10).

Profile	Sample ID	Lower boundary	Upper boundary	Layer	Macro Unit	N. phytoliths 1 g of sediment	Phytoliths weathering (%)	Multicelled phytoliths (%)
IBS	1	0	5	47	C	1.280.000	12.1	42.9
IBS	3	10	15	47	C	1.100.000	10.3	29.9
IBS	6	20	25	46	B1	2.030.000	6.6	27
IBS	8	30	35	42	B1	1.500.000	8.3	12.4
IBS	10	40	45	42	B1	1.200.000	6.8	5.5
IBS	13	55	60	48+33	B2	570.000	13.2	10.8
IBS	14	60	65	33	B2	640.000	13.2	19.6
IBS	16	70	75	33	B2	370.000	15.5	14.5
IBS	19	80	85	33+35	B2	900.000	7.9	14.5
IBS	21	90	100	28	B2	870.000	7.2	14.4
IBS	22	100	105	28+11	B2	840.000	5.7	12.8
IBS	24	110	115	11	B2	630.000	5.9	12.3
IBS	26	120	123	10	B2	760.000	10.3	12.9
IBS	28	130	140	7	B2	1.140.000	11.6	11.2
IBS	29	140	145	5	B2	1.020.000	4.9	19.7
IBS	30	145	150	5(+4)	B2	770.000	6.7	16.1
IBW	1	0	5	52	D	370.000	16.2	7.1
IBW	3	10	15	52	D	710.000	9.7	7
IBW	5	20	25	52	D	1.800.000	11.7	7.8
IBW	7	30	35	52	D	2.040.000	8.5	11.2
IBW	9	40	45	53	D	2.470.000	7.2	22.3
IBW	11	50	55	51	D	3.170.000	4.8	20.4
IBW	13	60	64	44	C	2.190.000	7.6	16.3
IBW	16	72	76	44	C	1.400.000	7.8	4.4
IBW	18	80	85	44	C	2.340.000	6.1	14.6
IBW	20	90	95	44	C	2.100.000	3.6	12.2
IBW	22	100	102	44	C	1.910.000	3	19.6
IBW	25	110	115	49+43	B1	1.790.000	4.3	16.9
IBW	27	120	125	46	B1	2.010.000	5.5	12.2
IBW	29	130	135	39	B1	1.800.000	5.5	15.7
IBW	31	140	145	39	B1	1.410.000	8.1	16.6
IBW	32	145	150	36	B1	850.000	9.2	8.4

Table 3. Description of samples and main phytolith results obtained from Ifri El Baroud trench V, South Profile (IBS) and West Profile (IBW) samples.

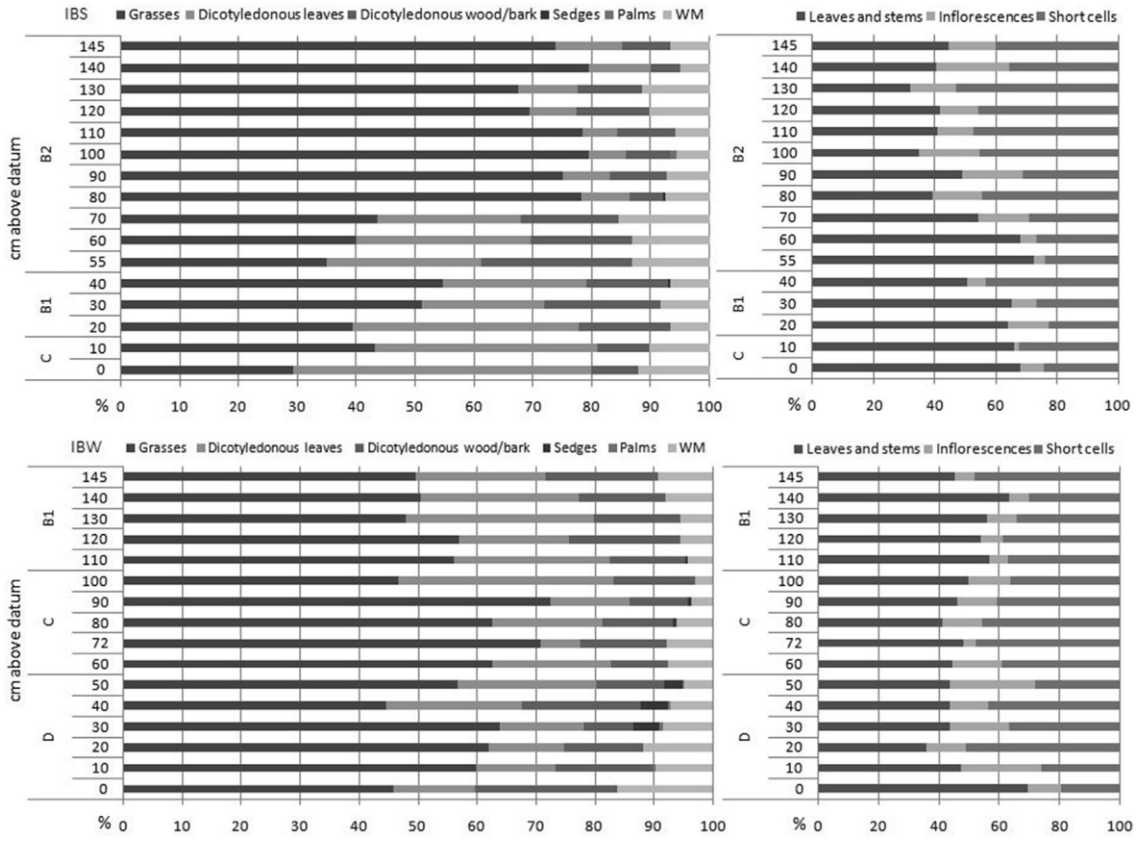

Fig. 10. Left: Relative abundances of phytoliths obtained from South Profile (IBS, top) and West Profile (IBW, bottom) samples. Right: anatomical origin of grass phytoliths.

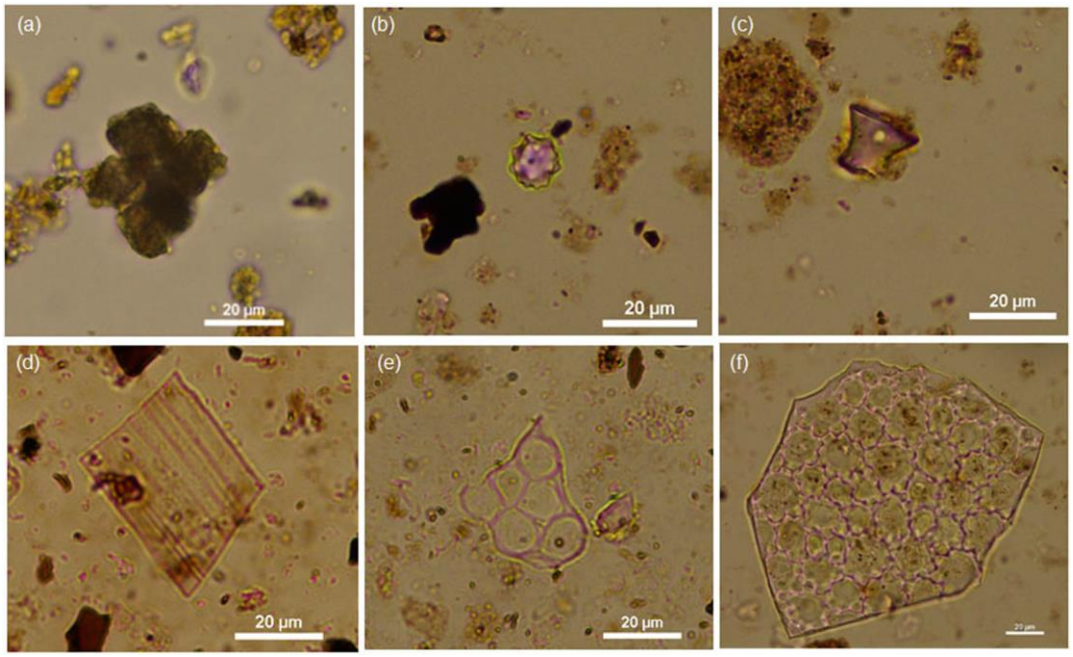

Fig. 11. Photomicrographs of opal phytoliths and calcitic microfossils identified in the samples (400x): (a) cluster of calcitic wood ash pseudomorphs; (b) spheroid echinate from the leaves of Arecaceae (palms); (c) short cell rondel from Pooideae grasses; (d) multicelled phytoliths from grass leaves/stems; (e) hair base from dicotyledonous leaves; (f) multicelled jigsaw-puzzle phytoliths from dicotyledonous leaves.

5.8. Macrofauna

Bones from the Escargotière layers (units B1 and B2) were for the most part well preserved thanks to the extreme dryness of the ashy sediments, while the material from the Couche rouge and lower levels (units C and D) was often covered by sediment crusts or highly fragmented, thus making the determination more challenging (Jentke, 2016).

In the faunal material of the four analysed sections (sub-squares G17a-d), more than 2600 vertebrate remains could be identified to the genus level, and in 2432 of cases, species could be determined (Table 4). Taphonomic evidence of cut-marks, percussion damage and thermal modification show that most of the faunal remains were brought and processed into the cave by humans. The fauna of larger vertebrates is mainly composed of mammalian remains, a large amount of ostrich eggshell fragments, remains of the freshwater turtle *Mauremys leprosa* and the terrestrial tortoise Testudo graeca, both representatives of larger reptiles.

The larger mammal fauna is characterized by medium to large ungulates like wild equid species (*Equus* sp.), Cuvier's Gazelle (*Gazella cuvieri*), Bubal Hartebeest (*Alcelaphus buselaphus*), and Aurochs (*Bos primigenius*). Today these taxa are known to inhabit open habitats or savannahs, which suggest that the environment at northeast Morocco was quite different from today (Michel et al., 2009; Mikdad et al., 2000). Due to climatic changes in this region all of these taxa have vanished from the study area today or have even gone completely extinct. It is interesting to note that the Bubal Hartebeest and the Aurochs, as the largest herbivores in faunal assemblage of Ifri El Baroud, only appear in unit B1 and B2. Nevertheless, the dominant mammal species throughout the whole section is the Barbary sheep (*Ammotragus lervia*). Since it does not need to drink from open waters and prefers to live in dryer mountainous habitats (Manlius, 2009; Wilson and Mittermeier, 2011), it still is found in some parts of Morocco today (Boitani et al., 1998). Carnivores are rare in the faunal assemblage and in 2015, only two species of the genus Panthera were identified from the nettoyage. Small game as hares, porcupine and turtles only appear in units B1 and B2, like the Bubal Hartebeest and the Aurochs (Table 4).

The amount of most represented prey species did not vary much over time, despite the considerable changes in environmental conditions of the Late Glacial period. Nevertheless, there is variation in the frequency, which may have been caused by

human activities or climate change. The largest accumulation of mammal remains is within unit B1, at < 15.5 cal BP. Furthermore, the frequencies of ostrich eggshells and mammal bone fragments both peak soon after the transition from Couche rouge (unit C) to the Escargotière (unit B1). This pattern is also known from other sites, like Ifri n'Ammar, where bones of larger mammals are more frequent in the late Iberomaurusian levels (Nami and Moser, 2010).

Class	**Oder**	**Family**	**Species**	***NISP 2015****				
				Nettoyage	**Unit B2**	**Unit B1**	**Unit C**	**Unit D**
Mammalia	Carnivora	Felidae	*Panthera leo*	1	–	–	–	–
			Panthera pardus	1	–	–	–	–
	Perissodactyla	Equidae	*Equus* sp.	–	19	6	4	2
	Artiodactyla	Bovidae	*Alcelaphus buselaphus*	–	6	3	–	–
			Gazella cuvieri	–	16	12	2	1
			Bos primigenius	–	2	2	–	1
			Ammotragus lervia	–	40	103	18	6
	Rodentia	Hystricidae	*Hystrix cristata*	–	–	1	–	–
	Lagomorpha	Leporidae	*Lepus capensis*	–	1	1	–	–
Aves	Struthioniformes	Struthionidae	*Struthio camelus*	–	430	1258	393	20
Reptilia	Testudines	Geoemydidae	*Mauremys leprosa*	–	100	–	–	–
		Testudinidae	*Testudo graeca*	–	14	–	–	–

Table 4. Occurrence and number of species in the faunal material from Ifri El Baroud trench V. NISP= Number of identified bones per species.

5.9. Microfauna and molluscs

The amount of flotation residue of sub-square G17b was high in the analysed column for the units B2 and B1 but sharply decreased in units C and D (Fig. 12). Shells were numerous and often complete in the upper units, but rare and fragmented in the lower units C and D. Gastropods identified within the sediment column of sub-square G17b were *Otala* cf. *lactea*, *Alabastrina alabastrites*, *Sphincterochila maroccana*, *Cernuella globuloidea*, *Xeroleuca turcica*, and *Rumina decollata*.

Remains of vertebrates were rare and very fragmented. Fragments of shrews (*Crocidura* sp.), elephant shrews (Petrosaltator rozeti), barbary squirrels (*Atlantoxerus getulus*), Maghreb dormouse (*Eliomys munbyanus*), jerboa (*Jaculus* cf. *jaculus*), North African gerbil (*Gerbillus campestris*), Moroccan jird (Meriones grandis), Algerian

mouse (Mus spretus), horseshoe bat (*Rhinolophus* sp.), small birds, geckos, lizards, and scincs were identified. Remains of Maghreb dormice were found only in the lower levels (spits 37 to 52).

The highest amounts of ostrich eggshells occurred at the boundary between the Escargotière and the Couche rouge (Fig. 12). The analysis of the microfauna and mollusc remains show also evidence of the climatic change that took place at the passage between Couche rouge (unit C) and Escargotière (unit B). The presence of the Maghreb dormouse *Eliomys munbyanus* in the layers of the Iberomaurusian units C and D indicates a semi-desert environment, as also suggested by a peak of mollusc remains of *Sphinterochila maroccana*, a highly heat-tolerant species (Fig.12). By contrast, the midden units B1 and B2 reflect more humid conditions with a higher occurrence of the snail *Otala* cf. lactea. Gerbils, jirids and mice are present in most periods.

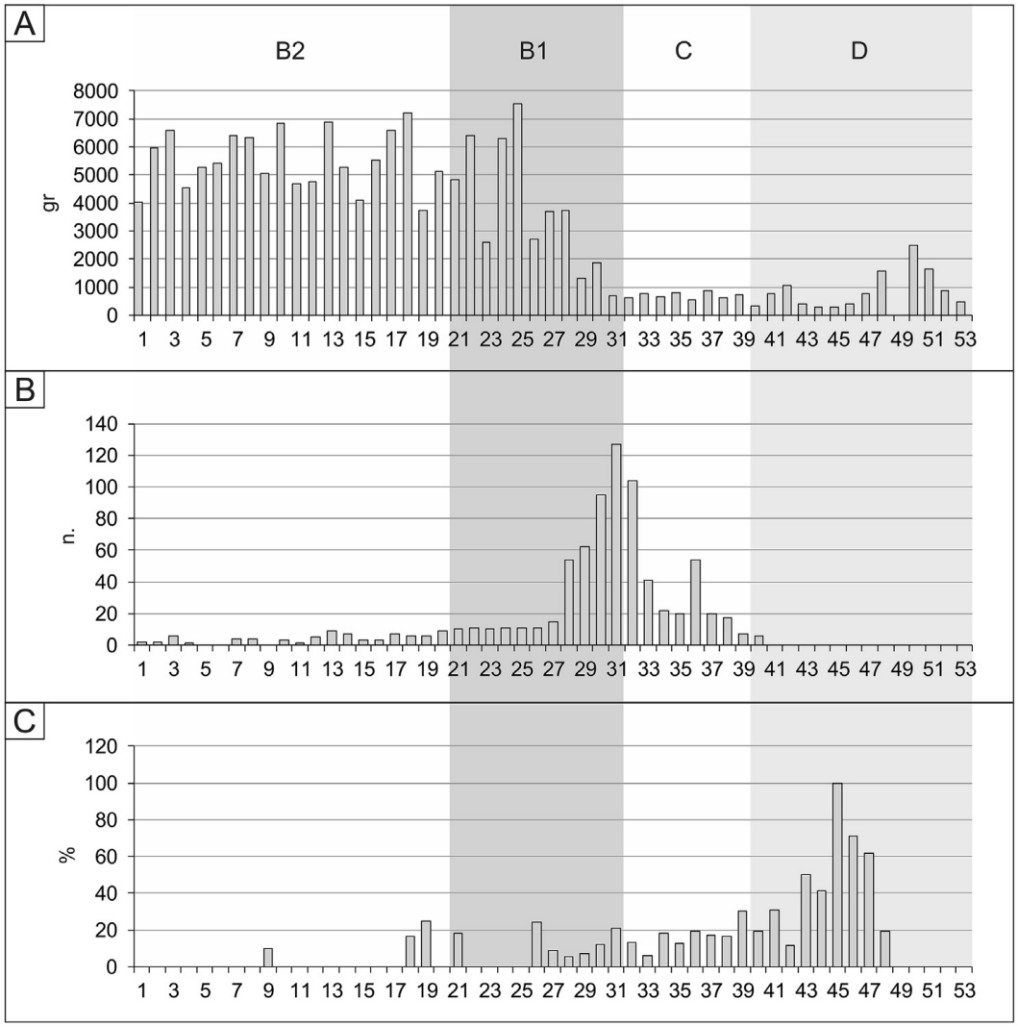

Fig. 12. (A) Flotation residue (in g) for the 53 samples from sub-square G17b. (B) Number of ostrich eggshells. (C) Number of *Sphincterochila* shells.

6. Discussion

6.1. Sediment accumulation, post-depositional alteration and general stratigraphy

The accumulation of the sedimentary and archaeological sequence took place through different depositional agents and natural or anthropogenic processes. The silty to sandy deposits of units C and D contain many allochthonous quartz grains, probably brought into the cave by eolian transport. Many fewer quartz grains are found in units B1 and B2, which reflects less eolian input under a more humid climate and denser vegetation cover during deposition of B1 and B2. Dispersed subangular limestone fragments originate from gravity driven roof spall and occur in all units, without any significant concentration in the sublayers. In units C and D, herbivore dung pellets and, more rarely, carnivore coprolites (Brönnimann et al., 2017a,b; Macphail and Goldberg, 2017) or fragments of such were detected. It is likely that the droppings were left by occasional visits of animals to the cave, and later dispersed into the sediment. Alternatively, they may have been unintentionally brought to the cave while attached to prey corpuses. The dung pellets at Ifri El Baroud are large in comparison to those found in the Palaeolithic sequence of Ifri n'Ammar rockshelter (Klasen et al., 2018). They probably originate from wild ruminants such as barbary sheep (Ammotragus lervia), the most dominant mammal species amongst the bone remains. The frequency of anthropogenic materials such as mollusc shells, bone and charcoal in units C and D are low in comparison to units B1 and B2; in the upper two units the anthropogenic sediment was mainly deposited by dumping and trampling shells after mollusc consumption. It is interesting that sediment lenses of entire snail shells are preserved, which may be explained by rapid burial during sediment accumulation. Sediment pockets of entire shells frequently occur in Holocene deposits of Ifri N'Etsedda (Linstädter et al., 2016), while they are rare in the sequence of Ifri Oudadane (Linstädter and Kehl, 2012).

Besides trampling, post-depositional alteration is indicated by diffuse phosphate enrichment of the groundmass or even phosphate encrustation. While part of the phosphorus likely derived from animal droppings, dissolution of apatite from animal bones may have provided another source. As noted above, bones from units C and D were often covered by sediment crusts or highly fragmented indicating a low degree of

preservation. In addition, the local accumulation of secondary carbonates points to dissolution and reprecipitation of carbonates. Besides the limestone roof of the cave, calcitic components of plant ash such as calcium oxalate and pseudomorphs of microcrystalline calcite (Canti and Brochier, 2017) occurring in ash lenses within units C and D probably represent the major source of secondary carbonates. Fine plant debris and abundant articulated phytoliths are peculiar components of the groundmass. They are locally found in dung pellets, but more often they occur in local concentrations within sublayers or larger sediment pockets of units C and D. The equal size of the plant fragments may be related to breakdown by trampling. Together with clear indications of partial burning, it is very likely that they derived from plant materials intentionally brought into the cave and used for covering of the cave floor as discussed below.

At Ifri El Baroud, no important stratigraphic disturbances have been recorded during fieldwork, except for slight contaminations of the superficial layers of unit B2 by historical or modern uses of the site. This has been mainly testified by the (limited) retrieval of small fragments of glass, goat droppings, and modern seeds within the first 15-20 cm of some of the excavated squares of trench V. However, the well-preserved layering argues against an effectual post-depositional mixing, and the presence of such modern implements could be the result of downwards movements of material through the loose uppermost snail-lenses or due to bounded bioturbations. Much more evident disturbances were identified during the excavation of trench IV in 1996, in particular in the eastern part of the excavated sector.

Post depositional mixing between stratigraphic units is considered to be unlikely, as confirmed by micromorphological analysis. Concerning the assemblages of lithics, it is noteworthy that no conjoins or refits have been found between units (except one single case between the uppermost layer of unit D and the lowermost layer of unit C), while several conjoins and refits have been found in each unit (Potì, 2017). Moreover, homogeneity of petrographical features has been observed in each assemblage (i.e. presence of blanks coming from the same core/raw material piece). Although each of the four main occupational phases (units D, C, B1 and B2) must be regarded as a palimpsest of different events (in terms of nature and intensity of human occupation), the internal variation of both archaeological and environmental data does not justify further inner divisions. Radiocarbon chronology itself indicates that - despite the thickness of the deposits - each sediment package (except unit C) accumulated quite

rapidly, and thus records relatively short phases of superimposed anthropogenic events (this seems to be particularity evident for unit B1). Such homogeneity in contextual evidence supports the maintenance of the macro division into four main units, which has no negative impact on the interpretation of the archaeological and stratigraphic significance of the sequence (Potì, 2017).

We observed that the limits between units C and B and, to a lesser extent, between units D and C are quite sharp, possibly documenting intervals of non-deposition or erosive truncation. Such features are accompanied by minor chronological gaps and seem therefore to suggest episodes of limited occupation or phases of abandonment of the site. The sedimentological transition between Couche rouge (units D-C) and Escargotière (units B1-B2) is dated to around 16-15 ka cal BP and seems to coincide with the transition from the cool and dry GS-2.1 including Heinrich Event 1 to the more favourable conditions of the GI-1 (Fig. 7). Many environmental indicators in and off-site provide evidence for an important landscape evolution over this period, which clearly had an important impact on the cultural dynamics. The chronological gap between the late Iberomaurusian (unit B) and the Epipalaeolithic-early Neolithic (unit A) is synchronous with the climatic and environmental worsening of the Younger Dryas.

From the point of view of archaeological features, layers of units C and D (early Iberomaurusian) present a finely laminated structure with thin concentrations of ash and charcoal separated by sandy micro-layers with sub-horizontal disposition. The finely laminated features with different compaction suggest that during this phase, human occupation occurred in continuous but brief and separate events. In contrast, the layers of units B1 and B2 (late Iberomaurusian) are thicker and provide signals of a much more pronounced human presence, with rich evidence of fire and accumulation of ash, snail shells and bones. Layers seems to have formed through a complex series of re-use (cut and fill) events, resulting from a constantly shifting human activity across the site, with frequent rejuvenation of living spaces. The large quantity of ash and the general abundance of anthropogenic materials suggest an intensification of activities and possibly a more continuous and prolonged occupation of the site or larger human groups. This seems to be confirmed by lithic technology (Potì, 2017). Although the layers can be rather thick, they are generally lens-shaped and are thus characterized by limited lateral extension, rarely more than few squares or sub-squares. The general

consistency of sediment properties (same components and consistency) and archaeological content all through the Escargotière does not support further internal differentiations and leads to consider units B1 and B2 as a quite homogeneous occupational "package" characterized by a uniform sedimentary evolutionary process. The chronology seems to confirm such observations.

The intensification of site use from around 16-15 ka cal BP with the rapid accumulation of massive Escargotière deposits represent the signal of a significant change in subsistence strategies and a diversification in resource exploitation after Heinrich Event 1 (HE1 acc. to Fletcher and Sánchez-Goñi, 2008). This period is also connected to the appearance of large cemeteries with elaborate mortuary practices in the region, as well as the evidence of systematic harvesting and processing of wild food resources (Humphrey et al., 2014). The emphasis on medium-large ungulates may be connected to local topography and/or to selective exploitation that involved efficient specialised hunting strategies. The spectrum of represented prey species did not vary much over time. Nevertheless, the enlargement of the hunting spectrum and the importance of small game and gastropods in the late Iberomaurusian layers highlights a change in the eating habits of the human groups during this period. From the current evidence, it appears that these shifts in human behaviour were tightly linked to the general trends in local palaeoenvironmental characteristics.

A similar change from fine yellow/reddish sandy sediments to overlying loose greyish midden deposits has been documented in other sites of the region such as Ifri n'Ammar and Taforalt, but also in Algeria further east, e.g. Abri Alain (Campmas et al., 2016).

6.2. Ifri El Baroud and other Iberomaurusian sites in northwest Africa

Based on the current evidence, the dates of the lower layers of unit D indicate Ifri El Baroud as one of the oldest Iberomaurusian evidence of the Maghreb. Nevertheless, it is important to note that the number of dated Iberomaurusian sites throughout northwest Africa is still limited.

At around at the same time as in Ifri El Baroud, the Iberomaurusian appeared in other three sites of the Oriental region of northeast Morocco: Taforalt, Ifri n'Ammar and Grotte du Rhafas. At Taforalt (Barton et al., 2013), bone and charcoal samples from the

early Iberomaurusian levels of the “Yellow series” date between ~22 and 15.9 ka cal BP (associable with units C and D of Ifri El Baroud), while the late Iberomaurusian phase of the “Grey series” falls between ~15 and 12,6 ka cal BP, contemporaneous with the midden unit B of Ifri El Baroud.

At Ifri n’Ammar, early Iberomaurusian layers produced an OSL date of 14.7 ± 0.9 ka (Klasen et al., 2018), well within the temporal range of the early Iberomaurusian of Ifri El Baroud. The uppermost layers of the Escargotière are dated between ~15.2 and 11.5 ka cal BP (Klasen et al., 2018; Moser, 2003), and perfectly match with the chronology of the late Iberomaurusian of Ifri El Baroud unit B.

Finally, in the outer part of Grotte du Rhafas (Doerschner et al., 2016), recent investigations have identified Iberomaurusian levels dated with OSL to 21400 ± 1500 (layer S3, early Iberomaurusian), and 15400 ± 1200 (layer S2, late Iberomaurusian).

Slightly younger chronologies come from the site of Kehf el Hammar in theWestern Rif (Bouzouggar et al., 2008) which yielded evidence of an early Iberomaurusian occupation (layers 6 to 4) dated to between ~19,1 and 16,7 ka cal BP, and associable with the early Iberomaurusian levels of Ifri El Baroud unit C. Evidences from layer 3 up to layer 1, supported by one radiocarbon date <16 ka cal BP and two TL dates, correlate with Iberomaurusian units B1-B2 of Ifri El Baroud.

Many other Moroccan sites only contain Iberomaurusian levels dated to the GI-1 and thus synchronous with the unit B occupation of Ifri El Baroud. This is the case for example of Bizmoune cave, Chaaba Bayda, Ghar Cahal, Hassi Ouenzga open air, Ifri Armas, Kehf Taht el Ghar, Marja, Pointe d'El Majni and Taghit Haddouch (Bouzouggar et al., 2008; Delibrias et al., 1982; Fernandez et al., 2015; Linstädter et al., 2012; Raynal and Occhietti, 2012; Wengler and Vernet, 1992).

Comparisons with Iberomaurusian contexts outside Morocco suggest that the Iberomaurusian layers of Ifri El Baroud are well comparable. At Afalou Bou Rhummel in Algeria, layer VII is dated ~18.5-17.7 ka cal BP (cf. unit C of Ifri El Baroud), while upper layers IV and III are calculated to fall between 14.5 and 12 ka cal BP (cf. unit B of Ifri El Baroud) (Hachi et al., 2002). Again, in Algeria, the site of Tamar Hat, recently re-dated (Hogue and Barton, 2016), provides the so far oldest Iberomaurusian deposit of northwest Africa with a stratigraphic succession dated between ~25.5 and 19.8 ka cal BP and potentially comparable with the initial evidences of Ifri El Baroud unit D.

In Libya at Haua Fteah, the earliest Iberomaurusian evidences are clustered between ~17.3 and 15.7 ka cal BP, likely parallel to Ifri El Baroud unit C. These early dates are followed by a greater number of evidences farther up in the sequence, ranging between 15.5 and 12 ka cal BP, in which Escargoti_ere-like layers rich in charcoals, snails, bones and lithics are recorded (cf. unit B of Ifri El Baroud) (Douka et al., 2014).

6.3. Human behaviours and local to regional palaeoenvironments as deduced from proxy data

Palaeoenvironmental data from the sequence of Ifri El Baroud, together with the contextual information from sedimentology and micromorphology, provide convincing indications of the local vegetation dynamic and environmental history during the early and late Iberomaurusian period. Specific behaviours of the human groups that inhabited the cave are also highlighted.

Anthracological data are indicative of a portion of past vegetation, as they reflect human harvesting of local species suitable to be used as fuel. Despite the long time interval analysed, the anthracological diagram of Ifri El Baroud does not show significant changes in firewood exploitation in the area around the cave. The entire sequence is characterized by the dominance of *Juniperus*/*Tetraclinis* and leguminous plants. The data reflects the dominance of a more arid and cooler climate than at present, a factor that explains the extension of open plant formations of heliophilous character. Despite the detection of slight nuances in the anthracological sequence of the site (increase of woody legume taxa at the end of the LGM and after the H1 event - beginning of the GI-1) (Carrión Marco et al., 2018), the continuity in both firewood gathering strategies and in the composition of local woody vegetation does not seem to reflect the environmental and sedimentary shift that mark the transition between early (units D and C) and late Iberomaurusian (unit B) levels, which took place during the transition from GS-2.1 to GI-1. This data contrasts the composition of pollen taxonomy, showing a very local picture of the exploited flora (including a probable anthropogenic bias in the firewood collection), while pollen includes other species at regional scale and reflects the dynamics of the vegetation both locally and regionally.

First results of the analysis of seeds and fruits shows the presence of species not recorded in the charcoal found at the site (Carrión Marco et al., 2018), and that these may have been collected for different purposes, other than for fuel. In the levels of units

D and C, the small seeds of wild legumes documented may have probably been gathered for consumption purposes, while seeds of *Juniperus* may have arrived together with the wood used as fuel. Within the Escargotière (units B1-B2), the presence of seeds of the genera *Vicia*, *Lathyrus* and *Lens* is quite interesting. These are wild annual legumes that produce large seeds with a high content of carbohydrates and proteins (Butler, 1998), and it is thus quite possible that they were collected as a subsistence resource. Seeds of *Vicia*, *Lathyrus* and *Lens* have also been documented in the late Iberomaurusian levels of Taforalt (Humphrey et al., 2014), as well as in Holocene layers at other sites of Morocco such as Ifri Oudadane and Kaf Taht el-Ghar (Morales, 2018). This confirms that these species could have been systematically exploited. Recent analyses of the oral health of human remains from Iberomaurusian and Capsian sites have shown a prevalence of caries suggesting a diet rich in carbohydrate-rich foods such as wild legumes (Groote et al., 2018; Humphrey et al., 2014). In addition to this, the presence of remains of Alfa grass (*Stipa tenacissima*) in both early and late Iberomaurusian layers, a perennial grass native to the western Mediterranean that is locally used as a source of fibre to produce nets, sandals, baskets etc., may reflect the use of herbaceous plants for such kind of uses (basketry, production of cords, clothing, and bedding).

The pollen analysis shows a very different vegetation pattern between the early (units D-C) and late Iberomaurusian levels (units B1-B2), which would characterize a stadial and interstadial period, respectively. During the early Iberomaurusian, the present thermo-Mediterranean bioclimatic belt of north-eastern Morocco was characterized by an open landscape dominated by a cold and arid steppe during GS-2.1, in which the main elements were heliophilous species adapted to the aforementioned climate. From a qualitative point of view, this vegetation was dominated by grasses (Poaceae), as well as by species of *Artemisia*, Chenopodiaceae and Resedaceae among herbs, and by *Ephedra fragilis* type and *Helianthemum* type among shrubs. Tree cover was very sparse. However, the continued presence of *Juniperus*/*Tetraclinis* and evergreen Quercus in this period confirms the existence of refuge areas for thermophilic flora (Cort_es-S_anchez et al., 2008). During the late Iberomaurusian, however, the study area was characterized by a relatively dense woodland cover of evergreen sclerophyllous oaks (mainly *Quercus coccifera* in the basins and Q. ilex in the surrounding mountains), arar tree (*Tetraclinis articulata*) or phoenician juniper

(*Juniperus phoenicea*), and probably some pine trees (*Pinus halepensis/pinea*). At this time, Holm oak (*Quercus ilex*) may have been abundant in the meso-Mediterranean bioclimatic belt, whereas fir (*Abies pinsapo*), deciduous oaks, *Pinus pinaster* and cedar (Cedrus atlantica) forest developed in the Rif mountains (Abel-Schaad et al., 2018; Cheddadi et al., 2009). Climate at this time may have been warm and humid, characteristic of the GI-1, as indicated by the importance of riparian forest (Fraxinus, Salix) and the xerothermophilous macchia composed mainly by *Pistacia lentiscus*, *Phillyrea*, *Rhamnus alaternus*, prickly cistus, heather, myrtle and shrub legumes, as well as by Ibero-African elements (*Periploca*, *Whitania*, *Ziziphus*). The greater abundance of anthropic elements (*Aster*, Cardueae, Cichorioideae) probably can be related to a greater use of the cave in this warmer and more humid period.

The phytolith accumulations observed are closely related to human activities carried out in the cave, mostly as fuel remains (wood and bark and perhaps mixed grasses and other monocotyledons such as sedges and palms possibly also related to matting and/or basketry, although these may have been introduced attached to woody fuel materials) and/or as grass bedding of occupational floors, as seems to be confirmed by embedded articulated multicelled phytoliths with sub-horizontal orientation in thin-sections. This is the case, for example, of the uppermost portion of unit C consisting of ashed plant material composed of articulated phytolith-rich assemblages derived from the epidermal tissues of dicotyledons and grass leaves and culms oriented subhorizontally in thin-section 202, suggested they derive from the burning of bedding. There is evidence for the use of grasses for bedding in the Late Pleistocene (Cabanes et al., 2010; Henry et al.,2004; Nadel et al., 2004; Rosen, 2003), but a similar pattern comes from the Middle Stone Age site of Sibudu Cave in South Africa, where repeated burnt bedding layers consisted mainly of sedges and other monocotyledons topped with aromatic, insecticidal and larvicidal dicotyledonous leaves reported as possibly burnt intentionally for cleaning or hygienic purposes (Goldberg et al., 2009; Wadley et al., 2011). These findings suggest that Iberomaurusian foragers used these plant materials as bedding surface preparation that could have been used for various purposes (sleeping, sitting, etc.) and could have been burned accidently at some point, or intentionally burnt, with critical implications regarding site use and maintenance of occupational surfaces, although further high-resolution analyses through simultaneous examination in

thin-section micromorphology and integrated microfossil evidence is required to confirm this pattern.

The environmental trend recognized at Ifri El Baroud is in more extended agreement with the regional and extra-regional palaeoenvironmental reconstruction as provided by the pollen records of marine and terrestrial archives. For the period of MIS 2 until ~15 ka cal BP, the pollen spectra of southern Mediterranean (Combourieu-Nebout et al., 2009; Desprat et al., 2013; Fletcher and Sánchez-Goñi, 2008; Langgut et al., 2011) indicate overall dry-cold conditions with an open steppe landscape dominated by taxa characteristic of arid and semi-desert environments (*Artemisia*, Ephedra, Cupressaceae), and xeric shrub formations with Cupressaceae and *Helianthemum*. The presence of *Pinus* and *Cedrus* indicates an association of the semi-desert taxa with a cedar-pine forest probably in the uplands, while scarce but continuous presence of *Quercus* - both deciduous and evergreen types - suggests only refuge populations for this genus (Combourieu-Nebout et al., 2009; Fletcher and Sánchez- Goñi, 2008; Langgut et al., 2011). Moreover, stronger arid conditions with sharp declines in moisture, considerable reduction in forest cover and expansion of arid and semi-desert vegetation are recorded during HE2 (~25-23.5 ka cal BP) and HE1 (~17-15.5 ka cal BP) (Fletcher and S_anchez-Go~ni, 2008; Langgut et al., 2011). After HE1, with the climate improvement and sea surface temperature (SST) warming of GI-1, palynological data suggests a rapid and large increase of Mediterranean pollen forest and a decline in steppe vegetation, indicating overall warmer and moister conditions (Langgut et al., 2011; Martrat et al., 2014; Moreno et al., 2004). During the Younger Dryas (~12.5-11.7 ka cal BP), a re-expansion of Artemisia and semidesert taxa together with the contraction of *Quercus* forest suggest the return to atmospheric dry and cold conditions synchronous with SST cooling (Combourieu-Nebout et al., 2009; Desprat et al., 2013).

Overall, much the same pattern is reflected in the few terrestrial pollen records so far available for the Late Glacial period. One of these is from Lake Ifrah (1610m a.s.l.) in the Middle Atlas in Morocco, which spans the period 29-5 ka cal BP (Cheddadi et al., 2009; Rhoujjati et al., 2010). Pollen data from a 9m long core confirm that until ~12 ka cal BP the landscape was dominated by *Artemisia*-rich steppe vegetation with Chenopodiaceae and Poaceae, and an arboreal cover reduced to less than 15% (Rhoujjati et al., 2010). During the harshest phases, January temperatures were generically 10º-15º cooler than today with only 300-400mm of precipitation per year

(Cheddadi et al., 2009). Nevertheless, pollen from pines, oaks and cedars, although in very low percentages, are present continuously throughout the sequence and values of Cedrus in particular arose between ~21 and 18 ka cal BP (Cheddadi et al., 2009). No major variations are recorded at Lake Ifrah during GI-1 and Younger Dryas, and only after the beginning of the Holocene did oak forests start to dominate the landscape at the expense of *Cedrus* and herbaceous plants (Rhoujjati et al., 2010).

The same results have been reached through the analysis of the recent AI.13 sediment core from Ait Ichou swamp in the southern part of the Middle Atlas (1560 m) (Tabel et al., 2016) and REM sediment core from Ras el Ma marsh in the central Middle Atlas (1633 m) (Nour El Bait et al., 2014), both showing high resilience of dominant steppe vegetation (*Artemisia*, Ephedra and Chenopodiaceae) and arid-cold conditions all through the Late Glacial until the early Holocene. The persistence of cold species (i.e. *Cedrus*) until the end of the Pleistocene and their rapid retreat with the increase of temperature during the early Holocene is also confirmed by the shorter pollen record of the mountainous site of Chataigneraie (~1000m a.s.l.) in north-eastern Algeria (Salamani, 1993). A model like Lake Ifrah is reported from the site of Garaat El-Ouez (45m a.s.l.) in the littoral marshes of El Kala in northwest Algeria, where the pollen diagram for the Late Glacial period documents open woodlands with *Pinus* and Poaceae associated with different steppe taxa (steppe-forest) and cedar (Benslama et al., 2010). The study of the long sedimentary sequence of Dar Fatma I (780m a.s.l.) in north-western Tunisia, confirms a first phase of the Late Glacial (after 20 ka) with *Abies*, *Cedrus* and *Pinus* in association with important values of Poaceae and other herbaceous species. In a later phase, synchronous with the GI-1, herbaceous pollen regressed (especially of Poaceae) while the frequency of *Alnus*, *Plantago* and *Quercus* increased (Ben Tiba and Reille, 1982; Stambouli-Essassi et al., 2007).

7. Conclusions

Overall, Ifri El Baroud provides a rich stratigraphic sequence featuring a well-preserved anthropogenic record. Based on current evidences, Epipalaeolithic-Neolithic deposits are only preserved in the innermost part of the cave. In contrast, in-situ Iberomaurusian layers have been identified in all sectors, down to a maximum depth of ~3m in trenches II and V.

Radiocarbon results for Ifri El Baroud reveal a high-resolution succession of interstratified human occupations. The Iberomaurusian archaeological layers span a period from roughly 23 to 13 ka cal BP and yield very rich lithic assemblages, as well as botanical and faunal remains. Following sedimentological differences and stratigraphic criteria, Iberomaurusian layers have been divided into four main sets of deposits separated by a sedimentary shift. Units C and D consist of packed laminated sandy sediments of brown to yellowish colour and correspond to the early Iberomaurusian occupation of the site. Units B1 and B2 consist in loosely packed ashy grey layers rich in terrestrial gastropod shells and correspond to the late Iberomaurusian occupation of the site. The small Epipalaeolithic-Neolithic sample (unit A), stratigraphically independent from the rest of the sequence, has not been discussed in detail within this paper.

From an archaeological perspective, no sterile layers have been detected at the site, but dating evidence indicates gaps between unit A and unit B, between unit B and unit C, within unit C, and to a lesser extent between unit C and D, thus revealing phases of nonsedimentation or erosion during possible events of abandonment of the site. When compared with the palaeoclimatic record, it is interesting to note that such sedimentary hiatuses chronologically coincide with episodes of abrupt deterioration of climate or are contemporaneous with important environmental shifts. In particular, the transition from Couche rouge (unit C) to Escargotière (unit B1) seems to have taken place during the transition from GS-2.1 (including Heinrich event 1) to GI-1, while the chronological hiatus between the late Iberomaurusian and the Epipalaeolithic unit A is synchronous with the climatic and environmental downturn of the Younger Dryas.

From the point of view of paleoenvironmental reconstruction, the analysis of samples from the whole sequence has permitted us to highlight the evolution of the local landscape and to find connections with what has been observed on a macro-regional scale. Our data suggest environmental changes from cold-arid conditions to comparatively warmer and moister conditions at the transition from the early to the late Iberomaurusian occupations. The differentiation seems to be supported by the sedimentological data and by shift of subsistence patterns and resource exploitation. In addition, our results indicate specific human behaviours connected to bedding of the living surfaces, plant fuel supply (i.e. selective exploitation of local flora) and animal resource exploitation.

Being one of the few sequences in the whole northwest Africa yielding both early and late Iberomaurusian layers, Ifri El Baroud assumes a role of critical importance in the understanding of the human and landscape ecology in the period between the LGM and the Younger Dryas.

Data availability

The methodology for the semiautomatic square allocation process is available at https://doi.org/10.17605/OSF.IO/J4VFC along with code and data.

CRediT authorship contribution statement

Alessandro Potì: Conceptualization, Investigation, Data curation, Writing - original draft, Visualization, Supervision, Writing - review & editing. Martin Kehl: Conceptualization, Formal analysis, Investigation, Writing - original draft, Visualization, Writing – review & editing. Manuel Broich: Investigation, Data curation, Visualization, Writing - review & editing. Yolanda Carrión Marco: Formal analysis, Investigation, Writing - original draft, Visualization, Writing - review & editing. Rainer Hutterer: Formal analysis, Investigation, Writing - original draft, Writing - review & editing. Thalia Jentke: Formal analysis, Investigation, Writing – original draft, Visualization, Writing - review & editing. Jörg Linstädter: Conceptualization,Writing - review & editing. José Antonio López- Sáez: Formal analysis, Investigation, Writing - original draft, Visualization, Writing - review & editing. Abdeslam Mikdad: Conceptualization, Writing - review & editing. Jacob Morales: Formal analysis, Investigation, Writing - original draft, Writing - review & editing. Sebastián Pérez-Díaz: Formal analysis, Investigation, Writing - review & editing. Marta Portillo: Formal analysis, Investigation, Writing - original draft, Visualization, Writing – review & editing. Clemens Schmid: Software, Formal analysis, Investigation, Data curation, Writing - original draft, Visualization, Writing - review & editing. Paloma Vidal-Matutano: Formal analysis, Investigation, Writing - original draft, Visualization, Writing - review & editing. Gerd-Christian Weniger: Conceptualization, Supervision, Project administration, Writing - review & editing.

Acknowledgments

Permission to carry out new field research at Ifri El Baroud and to export sediment and micromorphological samples was granted by the Institut National des Sciences de l'Archéologie et du Partimoine of Rabat, Morocco. The excavation was financially supported by the Deutsche Forschungsgemeinschaft (DFG, German Research Foundation) e Projekt nummer 57444011 - SFB 806. AMS Radiocarbon dates have been financed by the SFB 806 and the "Paleoplant" (ERC-CG-2013-SH6) Consolidator Grant. At the time of this research, AP was PhD candidate at the SFB 806 - University of Cologne. MP research has been funded by PALEOPLANT and EU Horizons 2020 MICROARCHAEODUNG (H2020-MSCA-IF-2015- 702529). YCM and JM are beneficiaries of a Ramón y Cajal research fellowship funded by the Spanish Ministerio de Economía, Industria y Competitividad. Part of the charcoal analysis was performed with the financial support of a research technician contract to PVM (CPI-16-432) funded by the additional budget from the Ramón y Cajal research programme. The authors wish to thank the anonymous reviewers for their valuable comments and Taylor Otto for the editing of the English language.

Appendix A. Supplementary data

Supplementary data to this article can be found online at https://doi.org/10.1016/j.quascirev.2019.07.013.

References

Abel-Schaad, D., Iriarte, E., López-Sáez, J.A., Pérez-Díaz, S., Sabariego, S., Cheddadi, R., Alba-Sánchez, F., 2018. Are *Cedrus atlantica* forests in the Rif mountains of Morocco heading towards local extinction? Holocene 28, 1023–1037.

Alba-Sánchez, F., Abel-Schaad, D., López-Sáez, J.A., Sabariego,, S., Pérez-Díaz, S., González, A., 2018. Paleobiogeografía de *Abies* spp. y *Cedrus atlantica* en el Mediterráneo Occidental (península Ibérica y Marruecos). Ecosistemas 27, 26–37.

Albert, R.M., Ruiz, J.A., Sans, A., 2016. PhytCore ODB: a new tool to improve efficiency in the management and exchange of information on phytoliths. Journal of Archaeological Science 68, 98–105.

Albert, R.M., Shahack-Gross, R., Cabanes, D., Gilboa, A., Lev-Yadun, S., Portillo, M., Sharon, I., Boaretto, E., Weiner S., 2008. Phytolith-rich Layers from the Late Bronze and Iron Ages at Tel Dor (Israel): Mode of Formation and Archaeological Significance. Journal of Archaeological Science 35, 57–75.

Albert, R.M., Weiner, S., 2001. Study of phytoliths in prehistoric ash layers using a quantitative approach. In: Meunier, J.D., Colin, F. (Eds.), Phytoliths, Applications in Earth Sciences and Human History. A.A. Balkema Publishers. Lisse, pp. 251–266.

Balout, L., 1955. Préhistoire de l'Afrique du Nord: essai de chronologie. Arts et Métiers Graphiques.

Barton, R.N.E., Bouzouggar, A., Collcutt, S.N., Carrión Marco, Y., Clark-Balzan, L., Debenham, N.C., Morales, J., 2016. Reconsidering the MSA to LSA transition at Taforalt Cave (Morocco) in the light of new multi-proxy dating evidence. Quaternary International 413, Part A, 36–49.

Barton, R.N.E., Bouzouggar, A., Hogue, J.T., Lee, S., Collcutt, S.N., Ditchfield, P., 2013. Origins of the Iberomaurusian NW Africa: New AMS radiocarbon dating of the Middle and Later Stone Age deposits at Taforalt Cave, Morocco. Journal of Human Evolution 65, 266–281.

Ben Tiba, B., Reille, M., 1982. Recherche pollenanlytiques dans les montagnes de Kroumirie (Tunisie Septentrionale) premiers résultats. Ecologia Mediterranea VIII (4), 76–86.

Ben-Ncer, A., 2004. Etude de la sépulture ibéromaurusienne 1 d'Ifri n'Baroud (Rif oriental, Maroc). Antropo 7, 177–185.

Benslama, M., Andrieu-Ponel, V., Guiter, F., Reille, M., Beaulieu, J.-L. de, Migliore, J., Djamali, M., 2010. Nouvelles contributions à l'histoire tardiglaciaire et holocène de la végétation en Algérie analyses polliniques de deux profils sédimentaires du complexe humide d'El-Kala. Comptes Rendus Biologies 333, 744–754.

Boitani, L., Corsi, F., De Biase, A., D'Inzillo Caranza, I., Ravagli, M., Reggiani, G., Sinibaldi, I., Trapanese, P., 1998. A databank for the conservation and management of the African mammals. Istituto di Ecologia Applicata, Rome, Italy.

Bouzouggar, A., Barton, R.N.E., Blockley, S., Bronk-Ramsey, C., Collcutt, S., Gale, R., 2008. Reevaluating the Age of the Iberomaurusian in Morocco. African Archaeological Review 25, 3–19.

Bozarth, S.R., 1992. Classification of phytoliths formed in selected dicotyledons native to the Great Plains. In: Rapp, G., Mulholand, S.C. (Eds.), Phytolith Systematics. Plenum Press, New York, pp. 193–214.

Brochier, J.E., Thinon, M., 2003. Calcite crystals, starch grains aggregates or…POCC? Comment on 'calcite crystals inside archaeological plant tissues'. Journal of Archaeological Science 30, 1211–1214.

Brönnimann, D., Ismail-Meyer, K., Rentzel, P., Pümpin, C., Lisá, L., 2017a. Excrements of Herbivores. In: Nicosia, C., Stoops, G. (Eds.), Archaeological Soil and Sediment Micromorphology. Wiley-Blackwell, Chichester, 55–66.

Brönnimann, D., Pümpin, C., Ismail-Meyer, K., Rentzel, P., Égüez, N., 2017b. Excrements of Omnivores and Carnivores. In: Nicosia, C., Stoops, G. (Eds.), Archaeological Soil and Sediment Micromorphology. Wiley-Blackwell, Chichester, 67–82.

Brown, D.A., 1984. Prospects and limits of a phytolith key for grasses in the central United States. Journal of Archaeological Science 11, 345–368.

Burgaz, M.E., Güemes, J. & Roselló, M.J., 1994. Estudios palinológicos de flora autóctona valenciana: Anacardiaceae, Capparaceae y Coriariaceae. In: La Serna-Ramos, I. (Ed.), Polen y Esporas: Contribución a su conocimiento. Universidad de La Laguna, Tenerife, pp. 9–18

Burjachs, F., López-Sáez, J.A., Iriarte, M.J., 2003. Metodología Arqueopalinológica. In: Buxó, R., Piqué, R. (Eds.) La recogida de muestras en Arqueobotánica: objetivos y propuestas metodológicas. La gestión de los recursos vegetales y la transformación del paleopaisaje en el Mediterráneo occidental, Museu d'Arqueologia de Catalunya, Barcelona, pp. 11–18.

Butler, A., 1998. Grain Legumes: evidence of these important ancient food resources from Early Pre-agrarian and Agrarian sites in Southwest Asia. In: Damania, A.B., Valkoun, J., Willcox, G., Qualset, C.O. (Eds.), The Origins of Agriculture and Crop Domestication. ICARDA, Aleppo, pp. 102–117.

Cabanes, D., Mallol, C., Expósito, I., Baena, J., 2010. Phytolith evidence for hearths and beds in the late Mousterian occupations of Esquilleu cave (Cantabria, Spain). Journal of Archaeological Science 37, 2947–2957.

Canti, M.G., 2003. Aspects of chemical and microscopic characteristics of plant ashes found in archaeological soils. Catena 54, 339–361.

Canti, M.G., Brochier, J.É., 2017. Plant Ash. In: Nicosia, C., Stoops, G. (Eds.), Archaeological Soil and Sediment Micromorphology. doi:10.1002/9781118941065.ch17.

Carrión, J.S., Navarro, C., Navarro, J., Munuera, M., 2000. The distribution of cluster pine (*Pinus pinaster*) in Spain as derived from palaeoecological data, relationships with phytosociological classification. Holocene 10, 243–252.

Carrión Marco, Y., Vidal-Matutano, P., Morales, J., Henríquez Valido, P., Potì, A., Kehl, M., Linstädter, J., Weniger, G.-C., Mikdad, A., 2018. Late Glacial Landscape Dynamics Based on Macrobotanical Data: Evidence From Ifri El Baroud (NE Morocco). Environmental Archaeology 573, 1–15. doi:10.1080/14614103.2018.1538088.

Charco, J., 1999. El bosque mediterráneo en el norte de África. Biodiversidad y lucha contra la desertificación. Agencia Española de Cooperación Internacional, Madrid.

Charco, J., 2001. Guía de los árboles y arbustos del norte de África. Agencia Española de Cooperación Internacional, Madrid.

Cheddadi, R., Fady, B., François, L., H.L., Suc, J.-P., Huang, K., Demarteau, M., Vendramin, G.G., Ortu, E., 2009. Putative glacial refugia of *Cedrus atlantica* deduced from Quaternary pollen records and modern genetic diversity. Journal of Biogeography 36, 1361–1371.

Combourieu-Nebout, N., Peyron, O., Dormoy, I., Desprat, S., Beaudouin, C., Kotthoff, U., Marret, F., 2009. Rapid climatic variability in the west Mediterranean during the last 25 000 years from high resolution pollen data. Climate of the Past 5(3), 503–521.

Cortés-Sánchez, M., Morales, A., Simón, M.D., Bergadà, M.M., Delgado, López-García, P., López-Sáez, J.A., Lozano, M.C., Riquelme, J.A., Roselló, E., Sánchez-Marco, A., Vera-Peláez, J.L., 2008. Paleoenvironmental and cultural dynamics of the coast of Málaga (Andalusia, Spain) during the Upper Pleistocene and early Holocene. Quaternary Science Reviews 27, 2176–2193.

Costa, M., Morla, C., Sainz, H., 2005. Los bosques ibéricos: Una interpretación geobotánica. Planeta, Barcelona.

Delibrias, G., Guillier, M.T., Labeyrie, J., 1982. GIF natural radiocarbon measurements IX. Radiocarbon 24(3), 291–343.

Desprat, S., Combourieu-Nebout, N., Essallami, L., Sicre, M.A., Dormoy, I., Peyron, O., Siani, G., Bout Roumazeilles, V., Turon, J.L., 2013. Deglacial and Holocene vegetation and climatic changes in the southern Central Mediterranean from a direct land–sea correlation. Clim. Past 9(2), 767–787. doi:10.5194/cp-9-767-2013.

Doerschner, N., Fitzsimmons, K.E., Ditchfield, P., McLaren, S.J., Steele, T.E., Zielhofer, C., McPherron, S.P., Bouzouggar, A., Hublin, J.-J., 2016. A New Chronology for Rhafas, Northeast Morocco, Spanning the North African Middle Stone Age through to the Neolithic. Plos One 11(9), e0162280. doi:10.1371/journal.pone.0162280.

Douka, K., Jacobs, Z., Lane, C., Grün, R., Farr, L., Hunt, C., Inglis, R.H., Reynolds, T., 2014. The chronostratigraphy of the Haua Fteah cave (Cyrenaica, northeast Libya). Journal of Human Evolution 66, 39–63.

Driesch, A. von den., 1976. Das Vermessen von Tierknochen aus vor- und frühgeschichtlichen Siedlungen. Institut Paläoanatomie Domestikation und Geschichte der Tiermedizin, München.

Evans, M.E., Heller, F., 2003. Environmental Magnetism : Principles and Applications of Enviromagnetics. International Geophysics Series, Academic Press, Amsterdam.

Fennane, M., Ibn-Tattou, M., Mathez, J., Ouyahya, A., El-Oualidi, J., 1999. Flore Pratique du Maroc, vol. 1. Institut Scientifique, Université Mohammed V, Rabat.

Fennane, M., Ibn-Tattou, M., Ouyahya, A., El-Oualidi, J., 2007. Flore Pratique du Maroc, vol. 2. Institut Scientifique, Université Mohammed V, Rabat.

Fennane, M., Ibn-Tattou, M., Ouyahya, A., El-Oualidi, J., 2014. Flore Pratique du Maroc, vol. 3. Institut Scientifique, Université Mohammed V, Rabat.

Fernandez, P., Bouzouggar, A., Collina-Girard, J., Coulon, M., 2015. The last occurrence of Megaceroides algericus Lyddekker, 1890 (Mammalia, Cervidae) during the middle Holocene in the cave of Bizmoune (Morocco, Essaouira region). Quaternary International 374, 154–167. doi:10.1016/j.quaint.2015.03.034.

Fletcher, W.J., Sánchez-Goñi, M.F., 2008. Orbital- and sub-orbital-scale climate impacts on vegetation of the western Mediterranean basin over the last 48,000 yr. Quaternary Research 70, 451–464.

Geis, J.W., 1973. Biogenic silica in selected species of deciduous angiosperms. Soil Science 116, 113–130.

Goldberg, P., Miller, C.E., Schiegl, S., Ligouis, B., Berna, F., Conard, N.J., Wadley, L., 2009. Bedding, hearths, and site maintenance in the Middle Stone Age of Sibudu Cave, KwaZulu-Natal, South Africa. Archaeological and Anthropological Sciences 1, 95–122.

Goody, P.C., 2004. Anatomie des Pferdes. 1. Aufl, Eugen Ulmer GmbH & Co.

Görsdorf, J., Eiwanger, J., 1999. Radiocarbon datings of late Palaeolithic, Epipalaeolithic and Neolithic sites in Northeastern Morocco. In: Evin, J., Oberlin, C., Daugas, J.-P., Salles, J.-F. (Eds.), 3ème Congrès International, 14C et Archéologie, Lyon 6-10 Avril 1998. Société Préhistorique Française, Paris, pp. 365–370.

Greguss, P., 1955. Identification of Living Gymnosperms on the Basis of Xylotomy. Akadémiai Kiado, Budapest.

Greguss, P., 1959. Holzanatomie der Europaïschen Laubhölzer und Straücher. Akadémiai Kiado, Budapest.

Groote, I. de, Morales, J., Humphrey, L., 2018. Oral health in Late Pleistocene and Holocene North West Africa. Journal of Archaeological Science: Reports. doi:10.1016/j.jasrep.2018.03.019.

Grimm, E.C., 1992. Tilia, version 2. Springfield. IL 62703. Illinois State Museum, Research and Collection Center, Springfield.

Grimm, E.C., 2004. TGView. Illinois State Museum, Springfield.

Grootes, P.M., Stuiver, M., White, J., Johnsen, S., Jouzel, J., 1993. Comparison of oxygen isotope records from the GISP2 and GRIP Greenland ice cores. Nature 366, 552–554. doi: 10.1038/366552a0.

Hachi, S., Fröhlich, F., Gendron-Badou, A., Lumley, H. de, Roubet, C., Abdessadok, S., 2002. Figurines du Paléolithique supérieur en matière minérale plastique cuite d'Afalou Bou Rhummel (Babors, Algérie). Premières analyses par spectroscopie d'absorption Infrarouge. L'Anthropologie 106, 57–97.

Henry, D.O., Hietala, H.J., Rosen, A.M., Demidenko, Y.E., Usik, V.I., Armagan, T.L., 2004. Human behavioral organization in the Middle Paleolithic were Neanderthals different? American Anthropologist 106, 17–31.

Hogue, J.T., Barton, R.N.E., 2016. New radiocarbon dates for the earliest Later Stone Age microlithic technology in Northwest Africa. Quaternary International 413, 62–75. doi:10.1016/j.quaint.2015.11.144.

Humphrey, L.T., Groote, I. de, Morales, J., Barton, R.N.E., Collcutt, S.N., Bronk-Ramsey, C., Bouzouggar, A., 2014. Earliest evidence for caries and eploitation of starchy plant foods in Pleistocene hunter-gatherers from Morocco. Proceedings of the National Academy of Sciences 111, 954–959.

Hutterer, R., Linstädter, J., Eiwanger, J., Mikdad, A., 2014. Human manipulation of terrestrial gastropods in Neolithic culture groups of NE Morocco. Quaternary International 320, 83–91.

Jacquiot, C., 1955. Atlas d'anatomie des bois des conifères. Cent. Tech. Bois., Paris.

Jacquiot, C., Trenard, D., Dirol., D., 1973. Atlas d'anatomie des bois des angiospermes (Essences feuillues). Cent. Tech. Bois., Paris.

Jenkins, E., 2009. Phytolith taphonomy: a comparison of dry ashing and acid extraction on the breakdown of conjoined phytoliths formed in *Triticum durum*. Journal of Archaeological Science 36, 2402–2407.

Jentke, T., 2016. Occurrence and temporal variation of larger vertebrates in the Iberomaurusian of NE Morocco, based on the Ifri El Baroud excavation 2015. Unpublished MA thesis, Rheinische Friedrich-Wilhelms-Universität Bonn.

Katz, O., Cabanes, D., Weiner, S., Maeir, A., Boaretto, E., Shahack-Gross, R., 2010. Rapid phytolith extraction for analysis of phytolith concentrations and assemblages during an excavation: An application at Tell es-Safi/Gath, Israel. Journal of Archaeological Science 37, 1557–1563.

Klasen, N., Kehl, M., Mikdad, A., Brückner, H., Weniger, G.-C., 2018. Chronology and formation processes of the Middle to Upper Palaeolithic deposits of Ifri n'Ammar using multi-method luminescence dating and micromorphology. Quaternary International 485, 89–102. doi:10.1016/j.quaint.2017.10.043.

Langgut, D., Almogi-Labin, A., Bar-Matthews, M., Weinstein-Evron, M., 2011. Vegetation and climate changes in the South Eastern Mediterranean during the Last Glacial-Interglacial cycle (86 ka): New marine pollen record. Quaternary Science Reviews 30(27-28), 3960–3972. doi:10.1016/j.quascirev.2011.10.016.

Linstädter, J., Eiwanger, J., Mikdad, A., Weniger, G.-C., 2012. Human occupation of Northwest Africa: A review of Middle Palaeolithic to Epipalaeolithic sites in Morocco. Quaternary International 274, 158–174.

Linstädter, J., Kehl, M., 2012. The Holocene archaeological sequence and site formation processes at Ifri Oudadane, NE Morocco. Journal of Archaeological Science 39, 3306–3323.

Linstädter, J., Kehl, M., Broich, M., López-Sáez, J.A., 2016. Chronostratigraphy, site formation processes and pollen record of Ifri n'Etsedda, NE Morocco. Quaternary International 406, 6–29

López-Sáez, J.A., Alba-Sánchez, F., López-Merino, L., Pérez-Díaz, S., 2010. Modern pollen analysis: a reliable tool for discriminating *Quercus rotundifolia* communities in Central Spain. Phytocoenologia 40, 57–72.

López-Sáez, J.A., Alba-Sánchez, F., Sánchez-Mata, D., Abel-Schaad, D., Gavilán, R.G., Pérez-Díaz, S., 2015. A palynological approach to the study of *Quercus pyrenaica* forest communities in the Spanish Central System. Phytocoenologia, 45, 107–124.

López-Sáez, J.A., Burjachs, F., López-García, P., López-Merino, L., 2006. Algunas precisiones sobre el muestreo e interpretación de los datos en Arqueopalinología. Polen, 15, 17–29.

López-Sáez, J.A., López-García, P., Burjachs, F., 2003. Arqueopalinología: Síntesis crítica. Polen 12, 5–35.

Macphail, R., Goldberg, P., 2017. Applied soils and micromorphology in archaeology (Cambridge Manuals in Archaeology). Cambridge University Press, Cambridge. doi:10.1017/9780511895562

Madella, M., Alexandre, A., Ball, T.B., ICPN Working Group, 2005. International Code for Phytolith Nomenclature 1.0. Annals of Botany 96, 253–260.

Manlius, N., 2009. Historical ecology and biogeography. An example: the Barbary Sheep (*Ammotragus lervia*) in Egypt. In: Riemer, H., Forster, F., Herb, M., Pöllath, N. (Eds.), Desert Animals in the Eastern Sahara: Desert Animals in the Eastern Sahara. Heinrich-Barth-Institut, Köln, pp. 111–128.

Martrat, B., Jimenez-Amat, P., Zahn, R., Grimalt, J.O., 2014. Similarities and dissimilarities between the last two deglaciations and interglaciations in the North Atlantic region. Quaternary Science Reviews 99, 122–134.

McBurney, C., 1967. The Haua Fteah (Cyrenaica) and the Stone Age of the South-East Mediterranean. Cambridge University Press, Cambridge.

Michel, P., Campmas, E., Stoetzel, E., Nespoulet, R., El Hajraoui, M.A., Amani, F., 2009. La macrofaune du Pléistocène supérieur d'El Harhoura 2 (Témara, Maroc): Données préliminaires. Anthropologie, Elsevier Masson 113 (2), 283–312.

Mikdad, A., Eiwanger, J., 1995. Programme du Rif Oriental. Rapport Préliminaire mission du 31 Mars 1995 au 30 Avril 1995. INSAP-KAVA, Bonn.

Mikdad, A., Eiwanger, J., Atki, H., Ben-Ncer, A., Bokbot, Y., Hutterer, R., Linstädter, J., Mouhsine, T., 2000. Recherches préhistoriques et protohistoriques dans le Rif oriental (Maroc): rapport préliminaire. Beiträge zur Allgemeinen und Vergleichenden Archäologie 20, 109–167.

Moore, P.D., Webb, J.A., Collinson, M.E., 1991. Pollen analysis. 2nd edition. Blackwell Scientific Publications, London.

Moreno, A., Cacho, I., Canals, M., Grimalt, J.O., Sanchez-Vidal, A., 2004. Millennial-scale variability in the productivity signal from the Alboran Sea record, Western Mediterranean Sea. Palaeogeography, Palaeoclimatology, Palaeoecology 211(3-4), 205–219. doi:10.1016/j.palaeo.2004.05.007.

Morales, J., 2018. The contribution of plant macro-remains to the study of wild plant consumption during the Later Stone Age and the Neolithic of north-western Africa. Journal of Archaeological Science: Reports. https://doi.org/10.1016/j.jasrep.2018.06.026

Moser, J., 2003. La Grotte d'Ifri n'Ammar: Tome 1: L'Ibéromaurusien. AVA-Forschungen 8. Linden Soft.

Mulholland, S.C., Rapp Jr, G., 1992. A morphological classification of grass silica-bodies. In: Rapp Jr., G., Mulholland, S.C. (Eds.), Phytolith Systematics: Emerging Issues, Advances in Archaeological and Museum Science. Plenum Press, New York, pp. 65–89.

Nadel, D., Weiss, E., Simchoni, O., Tsatskin, A., Danin, A., Kislev, M., 2004. Stone Age hut in Israel yields world's oldest evidence of bedding. Proceedings of the National Academy of Sciences 101, 6821–6826.

Nami, M., 2001. La grotte d'Ifri El Baroud: Etude d'une séquence ibéromaurusienne du Rif oriental (Maroc). Unpublished PhD thesis.

Nami, M., 2007. Les techno-complexes Ibéromaurusiens d'Ifri El Baroud (Rif Oriental, Maroc). Zeitschrift für Archäologie Außereuropäischer Kulturen 2, 183–239.

Nami, M., Moser, J., 2010. La Grotte d'Ifri n'Ammar; tome 2: Le Paléolithique Moyen. Forschungen zur Archäologie Außereuropäischer Kulturen (FAAK) 9, Reichert, Wiesbaden.

Neumann, K., Schoch W., Détienne, P., Schweingruber, F.H., Richter, H.G., 2001. Woods of the Sahara and the Sahel. Haupt, Bern.

Nour El Bait, M., Rhoujjati, A., Eynaud, F., Benkaddour, A., Dezileau, L., Wainer, K., Goslar, T., Khater, C., Tabel, J., Cheddadi, R., 2014. An 18 000-year pollen and sedimentary record from the cedar forests of the Middle Atlas, Morocco. Journal of Quaternary Science 29, 423–432.

Pales, L., Lambert, C., 1971. Atlas ostéologique pour server à l'identification des mammifères du quaternaire. Herbivores. Éditions du CNRS, 84 Pl., Paris.

Pallary, P., 1909. Instructions pour les recherches préhistoriques dans le Nord-Ouest de l'Afrique. Mémoires de la Société Historique Algérienne 3.

Peters, J., Van Neer, W., Plug, I. 1997. Comparative postcranial osteology of hartebeest (Al-celaphus buselaphus), Scimitar oryx (Oryx dammah) and Addax (Addax nasomacula-tus), with notes on the osteometry of Gemsbok (Oryx gazella) and Arabian Oryx (Oryx leucoryx). Koninklijk Museum voor Midden-Afrika. Annalen Zoologische Weten-schappen 280, 1–83.

Piperno, D.R., 2006. Phytoliths: A comprehensive guide for archaeologists and paleoecologists. AltaMira Press, Lanham.

Popesko, P., 2007. Atlas der topographischen Anatomie der Haustiere. Georg Thieme Verlag.

Portillo, M., Kadowaki, S., Nishiaki, Y., Albert, R.M., 2014. Early Neolithic household behavior at Tell Seker al-Aheimar (Upper Khabur, Syria): a comparison to ethnoarchaeological study of phytoliths and dung spherulites. Journal of Archaeological Science 42, 107–118.

Portillo, M., Belarte, M.C., Ramon, J., Kallala, N., Sanmartí, J., Albert, R.M., 2017a. An ethnoarchaeological study of livestock dung fuels from cooking installations in northern Tunisia. Quaternary International 431, 133–44.

Portillo, M., Llergo, Y., Ferrer, A., Albert, R.M., 2017b. Tracing microfossil residues of cereal processing in the archaeobotanical record: an experimental approach. Vegetation History Archaeobotany 26, 59–74.

Potì, A., 2017. Technical Change and Environmental Change in the Iberomaurusian: A Case Study from Ifri El Baroud, Morocco. Unpublished PhD thesis, University of Cologne.

Potì, A., Weniger, G.-C., in press. Human occupation of northern Morocco at the Last Glacial Maximum. In: Schmidt, I., Bicho, N., Weniger, G.-C., Cascalheira, J. (Eds.), Human adaptations to the Last Glacial Maximum: the Solutrean and its neighbours. Cambridge Scholars Publishing.

Rasmussen, S.O., Bigler, M., Blockley, S.P., Blunier, T., Buchardt, S.L., Clausen, H.B., Cvijanovic, I., Dahl-Jensen, D., Johnsen, S.J., Fischer, H., Gkinis, V., Guillevic, M., Hoek, W.Z., Lowe, J.J., Pedro, J.B., Popp, T., Seierstad, I.K., Steffensen, J.P.,

Svensson, A.M., Vallelonga, P., Vinther, B.M., Walker, M.J.C., Wheatley, J.J., Winstrup, M., 2014. A stratigraphic framework for abrupt climatic changes during the Last Glacial period based on three synchronized Greenland ice-core records: refining and extending the INTIMATE event stratigraphy. Quaternary Science Reviews 106, 14–28.

Raynal, J.-P., Occhietti, S., 2012. Amino Chronology and an Earlier Age for the Moroccan Aterian. In: Hublin, J.-J., McPherron, S.P. (Eds.), Modern Origins: A North African Perspective. Springer, New York, pp. 79–90.

Reille, M., 1992. Pollen et Spores d'Europe et d'Afrique du Nord. Laboratoire de Botanique Historique et Palynologie, Marseille.

Reimer, P.J., Bard, E., Bayliss, A., Beck, J.W., Blackwell, P.G., Bronk-Ramsey, C., Buck, C.E., Cheng, H., Edwards, R.L., Friedrich, M., Grootes, P.M., Guilderson, T.P., Haflidason, H., Hajdas, I., Hatté, C., Heaton, T.J., Hoffmann, D.L., Hogg, A.G., Hughen, K.A., Kaiser, K.F., Kromer, B., Manning, S.W., Niu, M., Reimer, R.W., Richards, D.A., Scott, E.M., Southon, J.R., Staff, R.A., Turney, C.S.M., van der Plicht, J., 2013. IntCal13 and Marine13 radiocarbon age calibration curves 0-50,000 years cal BP. Radiocarbon 55(4), 1869–1887.

Rhoujjati, A., Cheddadi, R., Taïeb, M., Baali, A., Ortu, E., 2010. Environmental changes over the past c. 29,000 years in the Middle Atlas (Morocco): A record from Lake Ifrah. Journal of Arid Environments 74, 737–745.

Rivas-Martínez, S., 1987. Memoria del mapa de series de vegetación de España. 1:400.000. I.C.O.N.A., Madrid.

Rosen, A.M., 2003. Middle Paleolithic plant exploitation: the microbotanical evidence. In: Henry, D.O. (Ed.), Neanderthals in the Levant. Behavioral Organization and the Beginnings of Human Modernity. Continuum, London, pp. 156–171.

Salamani, M., 1993. Premières données paléophytogéographiques du cèdre de l'Atlas (Cedrus atlantica) dans la région de Grande Kabylie (NE Algérie). Palynosciences 2, 147–155.

Schmid, C., 2019. Research Compendium for a Contribution to 'Human occupation and environmental change in the western Maghreb during the Last Glacial Maximum (LGM) and the Late Glacial. New evidence from the Iberomaurusian site Ifri El Baroud (northeast Morocco).'. doi:10.17605/OSF.IO/J4VFC.

Schweingruber, F.H., 1976. Mikroskopische Holzanatomie, Anatomie microscopique de bois. Birmensdorf: Institut féderal de recherches forestière, Zurcher AG.

Schweingruber, F.H., 1990. Anatomie europäischer Hölzer. Haupt, Bern.

Shillito, L.-M., 2011. Taphonomic observations of archaeological wheat phytoliths from Neolithic Çatalhöyük, Turkey, and the use of conjoined phytolith size as an indicator of water availability. Archaeometry 53, 631–641.

Stambouli-Essassi, S., Roche, E., Bouzid, S., 2007. Evolution de la végétation et du climat dans le Nord-ouest de la Tunisie au cours des 40 derniers millénaires. Geo-Eco-Trop 31, 171–214.

Stoops, G., 2003. Guidelines for the analysis and description of soil and regolith thin sections. Soil Science Society of America, Madison, WI, USA.

Tabel, J., Khater, C., Rhoujjati, A., Dezileau, L., Bouimetarhan, I., Carre, M., Vidal, L., Benkaddour, A., Nourelbait, M., Cheddadi, R., 2016. Environmental changes over the past 25 000 years in the southern Middle Atlas, Morocco. Journal of Quaternary Science 31, 93–102.

Tsartsidou, G., Lev-Yadun, S., Albert, R.M., Rosen, A.M., Efstratiou, N., Weiner, S., 2007. The phytolith archaeological record: strengths and weaknesses evaluated based on a quantitative modern reference collection from Greece. Journal of Archaeological Science 34, 1262–1275.

Tutin, T.G., Heywood, V.H., Burgues, N.A., Valentine, D.H., Walters, S.M., Webb, D.A., 1964. Flora Europaea. Cambridge University Press, Cambridge.

Twiss, P.C., 1992. Predicted world distribution of C_3 and C_4 grass phytoliths. In: G,.Rapp, Jr., S.C. Mulholland (Eds.), Phytolith Systematics: Emerging Issues, Advances in Archaeological and Museum Science. Plenum Press, New York, pp. 113–128.

Valdés, B., Díez, M.J., Fernández, I., 1987. Atlas polínico de Andalucía Occidental. Instituto de Desarrollo Regional nº 43, Universidad de Sevilla, Excma. Diputación de Cádiz, Sevilla.

Valdés, B., Montserrat, J.M., Font, X., 2006. A phytogeographical analysis of the N Moroccan flora. Willdenowia 36, 397–408.

Valdés, B., Rejdali, A., Achhal El Kadmiri, S., Juri, L., Montserrat, J.M., 2002. Catalogue des plantes vasculaires du Nord du Maroc incluant des clés d'identification. CSIC, Madrid.

Wadley, L., Sievers, C., Bamford, M., Goldberg, P., Berna, F., Miller, C., 2011. Middle Stone Age bedding construction and settlement patterns at Sibudu, South Africa. Science 334(6061), 1388–1391.

Wattez, J., Courty, M.A., 1987. Morphology of ash of some plant remains. In: Fédoroff, N., Bresson, L.M., Courty, M.A. (Eds.), Micromorphologie des sols – Soil Micromorphology. Association Francaise pour l'Étude du Sol, Plaisir, pp. 677–682.

Wengler, L., Vernet, J.-L., 1992. Vegetation, sedimentary deposits and climates during the Late Pleistocene and Holocene in eastern Morocco. Palaeogeography, Palaeoclimatology, Palaeoecology 94, 141–167.

Weninger, B., Joris, O., 2008. A 14C age calibration curve for the last 60 ka: the Greenland-Hulu U/Th timescale and its impact on understanding the Middle to Upper Paleolithic transition in Western Eurasia. Journal of Human Evolution 55(5), 772–781. doi:10.1016/j.jhevol.2008.08.017.

Wilson, D.E., Mittermeier, R.A., 2011. Handbook of the mammals of the world - Vol. 2. Hoofed mammals. Lynx Edicions, Barcelona.